CHAPTER

8 Waveguide Principles

In Chapter 6, we introduced transmission lines, and in Chapter 7, we studied their analysis. We learned that transmission lines are made up of two (or more) parallel conductors. In this chapter, we shall learn the principles of waveguides in which guiding of waves is accomplished by the bouncing of waves obliquely within the guide, as compared to the case of a transmission line in which the waves slide parallel to the conductors of the line.

We shall introduce waveguides by first considering a parallel-plate waveguide, that is, a waveguide consisting of two parallel, plane conductors and then extend it to the rectangular waveguide, which is a hollow metallic pipe of rectangular cross section, a common form of waveguide. We shall learn that waveguides are characterized by cutoff, which is the phenomenon of no propagation in a certain range of frequencies, and dispersion, which is the phenomenon of propagating waves of different frequencies possessing different phase velocities along the waveguide. In connection with the latter characteristic, we shall introduce the concept of group velocity. We shall also discuss the principles of cavity resonators, the microwave counterparts of resonant circuits, and of optical waveguides.

We shall study the topic of reflection and refraction of plane waves at an interface between two dielectrics, and finally introduce the dielectric slab waveguide, based on the phenomenon of total internal reflection at the interface, when the angle of incidence of the wave on the interface is greater than a certain critical value.

8.1 UNIFORM PLANE WAVE PROPAGATION IN AN ARBITRARY DIRECTION

In Chapter 4, we introduced the uniform plane wave propagating in the z-direction by considering an infinite plane current sheet lying in the xy-plane. If the current sheet lies in a plane making an angle to the xy-plane, the uniform plane wave would then propagate in a direction different from the z-direction. Thus, let us consider a uniform plane wave propagating in the z'-direction making an angle θ with the negative x-axis, as shown in Figure 8.1. Let the electric field of the wave be entirely in the y-direction. The magnetic field would then be directed as shown in the figure so that $\mathbf{E} \times \mathbf{H}$ points in the z'-direction.

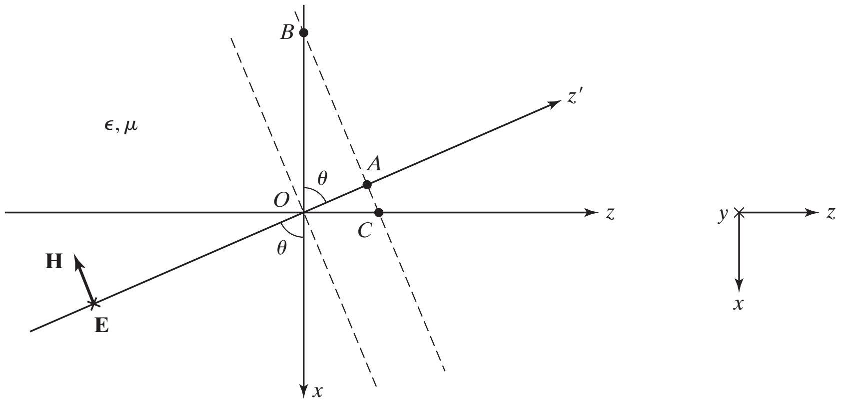

FIGURE 8.1

Uniform plane wave propagating in the z'-direction lying in the xz-plane and making an angle θ with the negative x-axis.

We can write the expression for the electric field of the wave as

$$\mathbf{E} = E_0 \cos(\omega t - \beta z')\, \mathbf{a}_y \tag{8.1}$$

where $\beta = \omega\sqrt{\mu\epsilon}$ is the phase constant, that is, the rate of change of phase with distance along the z'-direction for a fixed value of time. From the construction of Figure 8.2(a), we, however, have

$$z' = -x \cos\theta + z \sin\theta \tag{8.2}$$

so that

$$\begin{aligned} \mathbf{E} &= E_0 \cos[\omega t - \beta(-x\cos\theta + z\sin\theta)]\, \mathbf{a}_y \\ &= E_0 \cos[\omega t - (-\beta\cos\theta)x - (\beta\sin\theta)z]\, \mathbf{a}_y \\ &= E_0 \cos(\omega t - \beta_x x - \beta_z z)\, \mathbf{a}_y \end{aligned} \tag{8.3}$$

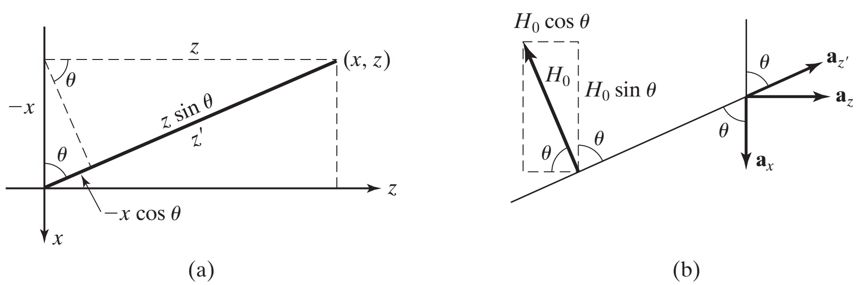

FIGURE 8.2

Constructions pertinent to the formulation of the expressions for the fields of the uniform plane wave of Figure 8.1.

where $\beta_x = -\beta \cos\theta$ and $\beta_z = \beta \sin\theta$ are the phase constants in the positive x- and positive z-directions, respectively.

We note that $|\beta_x|$ and $|\beta_z|$ are less than β, the phase constant along the direction of propagation of the wave. This can also be seen from Figure 8.1, in which two constant phase surfaces are shown by dashed lines passing through the points O and A on the z'-axis. Since the distance along the x-direction between the two constant phase surfaces, that is, the distance OB is equal to $OA/\cos\theta$, the rate of change of phase with distance along the x-direction is equal to

$$\beta\frac{OA}{OB} = \frac{\beta(OA)}{OA/\cos\theta} = \beta\cos\theta$$

The minus sign for β_x simply signifies the fact that insofar as the x-axis is concerned, the wave is progressing in the negative x-direction. Similarly, since the distance along the z-direction between the two constant phase surfaces, that is, the distance OC is equal to $OA/\sin\theta$, the rate of change of phase with distance along the z-direction is equal to

$$\beta\frac{OA}{OC} = \frac{\beta(OA)}{OA/\sin\theta} = \beta\sin\theta$$

Since the wave is progressing along the positive z-direction, β_z is positive. We further note that

$$\beta_x^2 + \beta_z^2 = (-\beta\cos\theta)^2 + (\beta\sin\theta)^2 = \beta^2 \tag{8.4}$$

and that

$$-\cos\theta\,\mathbf{a}_x + \sin\theta\,\mathbf{a}_z = \mathbf{a}_{z'} \tag{8.5}$$

where $\mathbf{a}_{z'}$ is the unit vector directed along z'-direction, as shown in Figure 8.2(b). Thus, the vector

$$\boldsymbol{\beta} = (-\beta\cos\theta)\mathbf{a}_x + (\beta\sin\theta)\mathbf{a}_z = \beta_x\mathbf{a}_x + \beta_z\mathbf{a}_z \tag{8.6}$$

defines completely the direction of propagation and the phase constant along the direction of propagation. Hence, the vector $\boldsymbol{\beta}$ is known as the *propagation vector.*

The expression for the magnetic field of the wave can be written as

$$\mathbf{H} = \mathbf{H}_0\cos(\omega t - \beta z') \tag{8.7}$$

where

$$|\mathbf{H}_0| = \frac{E_0}{\sqrt{\mu/\epsilon}} = \frac{E_0}{\eta} \tag{8.8}$$

since the ratio of the electric field intensity to the magnetic field intensity of a uniform plane wave is equal to the intrinsic impedance of the medium. From the construction in Figure 8.2(b), we observe that

$$\mathbf{H}_0 = H_0(-\sin\theta\,\mathbf{a}_x - \cos\theta\,\mathbf{a}_z) \tag{8.9}$$

Thus, using (8.9) and substituting for z' from (8.2), we obtain

$$\begin{aligned}\mathbf{H} &= H_0(-\sin\theta\,\mathbf{a}_x - \cos\theta\,\mathbf{a}_z)\cos[\omega t - \beta(-x\cos\theta + z\sin\theta)] \\ &= -\frac{E_0}{\eta}(\sin\theta\,\mathbf{a}_x + \cos\theta\,\mathbf{a}_z)\cos[\omega t - \beta_x x - \beta_z z] \qquad (8.10)\end{aligned}$$

Generalizing the foregoing treatment to the case of a uniform plane wave propagating in a completely arbitrary direction in three dimensions, as shown in Figure 8.3, and characterized by phase constants β_x, β_y, and β_z in the x-, y-, and z-directions, respectively, we can write the expression for the electric field as

$$\begin{aligned}\mathbf{E} &= \mathbf{E}_0\cos(\omega t - \beta_x x - \beta_y y - \beta_z z + \phi_0) \\ &= \mathbf{E}_0\cos[\omega t - (\beta_x\mathbf{a}_x + \beta_y\mathbf{a}_y + \beta_z\mathbf{a}_z)\cdot(x\mathbf{a}_x + y\mathbf{a}_y + z\mathbf{a}_z) + \phi_0] \\ &= \mathbf{E}_0\cos(\omega t - \boldsymbol{\beta}\cdot\mathbf{r} + \phi_0) \qquad (8.11)\end{aligned}$$

where

$$\boldsymbol{\beta} = \beta_x\mathbf{a}_x + \beta_y\mathbf{a}_y + \beta_z\mathbf{a}_z \qquad (8.12)$$

is the propagation vector,

$$\mathbf{r} = x\mathbf{a}_x + y\mathbf{a}_y + z\mathbf{a}_z \qquad (8.13)$$

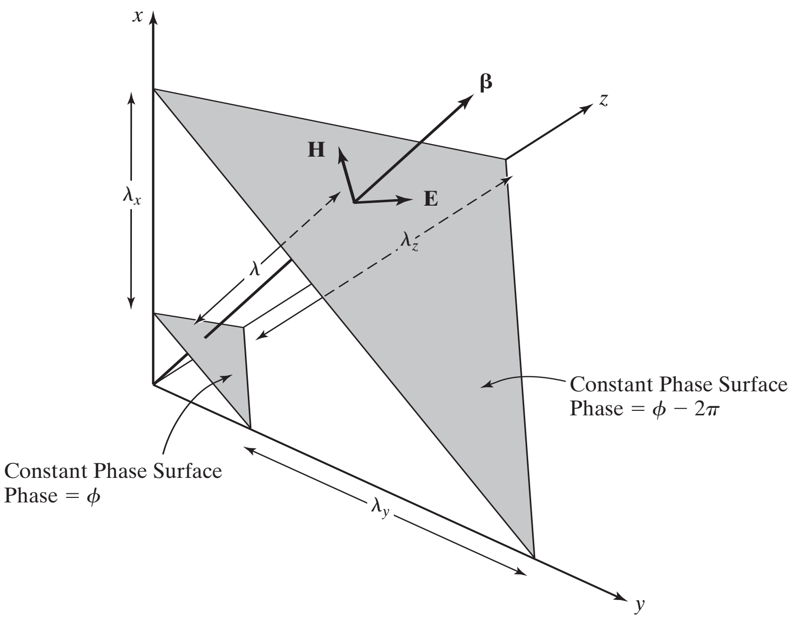

FIGURE 8.3

The various quantities associated with a uniform plane wave propagating in an arbitrary direction.

is the position vector, and ϕ_0 is the phase at the origin at $t = 0$. The position vector is the vector drawn from the origin to the point (x, y, z) and hence has components x, y, and z along the x-, y-, and z-axes, respectively. The expression for the magnetic field of the wave is then given by

$$\mathbf{H} = \mathbf{H}_0 \cos(\omega t - \boldsymbol{\beta}\cdot\mathbf{r} + \phi_0) \tag{8.14}$$

where

$$|\mathbf{H}_0| = \frac{|\mathbf{E}_0|}{\eta} \tag{8.15}$$

Since $\mathbf{E}$, $\mathbf{H}$, and the direction of propagation are mutually perpendicular to each other, it follows that

$$\mathbf{E}_0\cdot\boldsymbol{\beta} = 0 \tag{8.16a}$$

$$\mathbf{H}_0\cdot\boldsymbol{\beta} = 0 \tag{8.16b}$$

$$\mathbf{E}_0\cdot\mathbf{H}_0 = 0 \tag{8.16c}$$

In particular, $\mathbf{E} \times \mathbf{H}$ should be directed along the propagation vector $\boldsymbol{\beta}$ as illustrated in Figure 8.3, so that $\boldsymbol{\beta} \times \mathbf{E}_0$ is directed along $\mathbf{H}_0$. We can therefore combine the facts (8.16) and (8.15) to obtain

$$\begin{aligned}\mathbf{H}_0 &= \frac{\mathbf{a}_\beta \times \mathbf{E}_0}{\eta} = \frac{\mathbf{a}_\beta \times \mathbf{E}_0}{\sqrt{\mu/\epsilon}} = \frac{\omega\sqrt{\mu\epsilon}\,\mathbf{a}_\beta \times \mathbf{E}_0}{\omega\mu} \\ &= \frac{\beta\mathbf{a}_\beta \times \mathbf{E}_0}{\omega\mu} = \frac{\boldsymbol{\beta} \times \mathbf{E}_0}{\omega\mu}\end{aligned} \tag{8.17}$$

where $\mathbf{a}_\beta$ is the unit vector along $\boldsymbol{\beta}$. Thus,

$$\mathbf{H} = \frac{1}{\omega\mu}\boldsymbol{\beta} \times \mathbf{E} \tag{8.18}$$

Returning to Figure 8.3, we can define several quantities pertinent to the uniform plane wave propagation in an arbitrary direction. The apparent wavelengths λ_x, λ_y, and λ_z along the coordinate axes x, y, and z, respectively, are the distances measured along those respective axes between two consecutive constant phase surfaces between which the phase difference is 2π, as shown in the figure, at a fixed time. From the interpretations of β_x, β_y, and β_z as being the phase constants along the x-, y-, and z-axes, respectively, we have

$$\lambda_x = \frac{2\pi}{\beta_x} \tag{8.19a}$$

$$\lambda_y = \frac{2\pi}{\beta_y} \tag{8.19b}$$

$$\lambda_z = \frac{2\pi}{\beta_z} \tag{8.19c}$$

We note that the wavelength λ along the direction of propagation is related to λ_x, λ_y, and λ_z in the manner

$$\frac{1}{\lambda^2} = \frac{1}{(2\pi/\beta)^2} = \frac{\beta^2}{4\pi^2} = \frac{\beta_x^2 + \beta_y^2 + \beta_z^2}{4\pi^2}$$
$$= \frac{1}{\lambda_x^2} + \frac{1}{\lambda_y^2} + \frac{1}{\lambda_z^2} \tag{8.20}$$

The apparent phase velocities v_{px}, v_{py}, and v_{pz} along the x-, y-, and z-axes, respectively, are the velocities with which the phase of the wave progresses with time along the respective axes. Thus,

$$v_{px} = \frac{\omega}{\beta_x} \tag{8.21a}$$

$$v_{py} = \frac{\omega}{\beta_y} \tag{8.21b}$$

$$v_{pz} = \frac{\omega}{\beta_z} \tag{8.21c}$$

The phase velocity v_p along the direction of propagation is related to v_{px}, v_{py}, and v_{pz} in the manner

$$\frac{1}{v_p^2} = \frac{1}{(\omega/\beta)^2} = \frac{\beta^2}{\omega^2} = \frac{\beta_x^2 + \beta_y^2 + \beta_z^2}{\omega^2}$$
$$= \frac{1}{v_{px}^2} + \frac{1}{v_{py}^2} + \frac{1}{v_{pz}^2} \tag{8.22}$$

The apparent wavelengths and phase velocities along the coordinate axes are greater than the actual wavelength and phase velocity, respectively, along the direction of propagation of the wave. This fact can be understood physically by considering, for example, water waves in an ocean striking the shore at an angle. The distance along the shoreline between two successive crests is greater than the distance between the same two crests measured along a line normal to the orientation of the crests. Also, an observer has to run faster along the shoreline in order to keep pace with a particular crest than he has to do in a direction normal to the orientation of the crests. We shall now consider an example.

Example 8.1

Let us consider a 30-MHz uniform plane wave propagating in free space and given by the electric field vector

$$\mathbf{E} = 5(\mathbf{a}_x + \sqrt{3}\mathbf{a}_y) \cos [6\pi \times 10^7 t - 0.05\pi(3x - \sqrt{3}y + 2z)] \text{ V/m}$$

Then comparing with the general expression for **E** given by (8.11), we have

$$\begin{aligned}
\mathbf{E}_0 &= 5(\mathbf{a}_x + \sqrt{3}\mathbf{a}_y) \\
\boldsymbol{\beta} \cdot \mathbf{r} &= 0.05\pi(3x - \sqrt{3}y + 2z) \\
&= 0.05\pi(3\mathbf{a}_x - \sqrt{3}\mathbf{a}_y + 2\mathbf{a}_z) \cdot (x\mathbf{a}_x + y\mathbf{a}_y + z\mathbf{a}_z) \\
\boldsymbol{\beta} &= 0.05\pi(3\mathbf{a}_x - \sqrt{3}\mathbf{a}_y + 2\mathbf{a}_z) \\
\boldsymbol{\beta} \cdot \mathbf{E}_0 &= 0.05\pi(3\mathbf{a}_x - \sqrt{3}\mathbf{a}_y + 2\mathbf{a}_z) \cdot 5(\mathbf{a}_x + \sqrt{3}\mathbf{a}_y) \\
&= 0.25\pi(3 - 3) = 0
\end{aligned}$$

Hence, (8.16a) is satisfied; $\mathbf{E}_0$ is perpendicular to $\boldsymbol{\beta}$.

$$\beta = |\boldsymbol{\beta}| = 0.05\pi|3\mathbf{a}_x - \sqrt{3}\mathbf{a}_y + 2\mathbf{a}_z| = 0.05\pi\sqrt{9 + 3 + 4} = 0.2\pi$$

$$\lambda = \frac{2\pi}{\beta} = \frac{2\pi}{0.2\pi} = 10 \text{ m}$$

This does correspond to a frequency of $(3 \times 10^8)/10$ Hz or 30 MHz in free space. The direction of propagation is along the unit vector

$$\mathbf{a}_\beta = \frac{\boldsymbol{\beta}}{|\boldsymbol{\beta}|} = \frac{3\mathbf{a}_x - \sqrt{3}\mathbf{a}_y + 2\mathbf{a}_z}{\sqrt{9 + 3 + 4}} = \frac{3}{4}\mathbf{a}_x - \frac{\sqrt{3}}{4}\mathbf{a}_y + \frac{1}{2}\mathbf{a}_z$$

From (8.17),

$$\begin{aligned}
\mathbf{H}_0 &= \frac{1}{\omega\mu_0}\boldsymbol{\beta} \times \mathbf{E}_0 \\
&= \frac{0.05\pi \times 5}{6\pi \times 10^7 \times 4\pi \times 10^{-7}}(3\mathbf{a}_x - \sqrt{3}\mathbf{a}_y + 2\mathbf{a}_z) \times (\mathbf{a}_x + \sqrt{3}\mathbf{a}_y) \\
&= \frac{1}{96\pi}\begin{vmatrix} \mathbf{a}_x & \mathbf{a}_y & \mathbf{a}_z \\ 3 & -\sqrt{3} & 2 \\ 1 & \sqrt{3} & 0 \end{vmatrix} \\
&= \frac{1}{48\pi}(-\sqrt{3}\mathbf{a}_x + \mathbf{a}_y + 2\sqrt{3}\mathbf{a}_z)
\end{aligned}$$

Thus,

$$\mathbf{H} = \frac{1}{48\pi}(-\sqrt{3}\mathbf{a}_x + \mathbf{a}_y + 2\sqrt{3}\mathbf{a}_z) \cos [6\pi \times 10^7 t - 0.05\pi(3x - \sqrt{3}y + 2z)] \text{ A/m}$$

To verify the expression for **H** just derived, we note that

$$\begin{aligned}
\mathbf{H}_0 \cdot \boldsymbol{\beta} &= \left[\frac{1}{48\pi}(-\sqrt{3}\mathbf{a}_x + \mathbf{a}_y + 2\sqrt{3}\mathbf{a}_z)\right] \cdot [0.05\pi(3\mathbf{a}_x - \sqrt{3}\mathbf{a}_y + 2\mathbf{a}_z)] \\
&= \frac{0.05}{48}(-3\sqrt{3} - \sqrt{3} + 4\sqrt{3}) = 0
\end{aligned}$$

$$\begin{aligned}
\mathbf{E}_0 \cdot \mathbf{H}_0 &= 5(\mathbf{a}_x + \sqrt{3}\mathbf{a}_y) \cdot \frac{1}{48\pi}(-\sqrt{3}\mathbf{a}_x + \mathbf{a}_y + 2\sqrt{3}\mathbf{a}_z) \\
&= \frac{5}{48\pi}(-\sqrt{3} + \sqrt{3}) = 0 \\
\frac{|\mathbf{E}_0|}{|\mathbf{H}_0|} &= \frac{5|\mathbf{a}_x + \sqrt{3}\mathbf{a}_y|}{(1/48\pi)| - \sqrt{3}\mathbf{a}_x + \mathbf{a}_y + 2\sqrt{3}\mathbf{a}_z|} = \frac{5\sqrt{1+3}}{(1/48\pi)\sqrt{3+1+12}} \\
&= \frac{10}{1/12\pi} = 120\pi = \eta_0
\end{aligned}$$

Hence, (8.16b), (8.16c), and (8.15) are satisfied.

Proceeding further, we find that

$$\begin{aligned}
\beta_x &= 0.05\pi \times 3 = 0.15\pi \\
\beta_y &= -0.05\pi \times \sqrt{3} = -0.05\sqrt{3}\pi \\
\beta_z &= 0.05\pi \times 2 = 0.1\pi
\end{aligned}$$

We then obtain

$$\begin{aligned}
\lambda_x &= \frac{2\pi}{\beta_x} = \frac{2\pi}{0.15\pi} = \frac{40}{3}\text{ m} = 13.333\text{ m} \\
\lambda_y &= \frac{2\pi}{|\beta_y|} = \frac{2\pi}{0.05\sqrt{3}\pi} = \frac{40}{\sqrt{3}}\text{ m} = 23.094\text{ m} \\
\lambda_z &= \frac{2\pi}{\beta_z} = \frac{2\pi}{0.1\pi} = 20\text{ m} \\
v_{px} &= \frac{\omega}{\beta_x} = \frac{6\pi \times 10^7}{0.15\pi} = 4 \times 10^8\text{ m/s} \\
v_{py} &= \frac{\omega}{|\beta_y|} = \frac{6\pi \times 10^7}{0.05\sqrt{3}\pi} = 4\sqrt{3} \times 10^8\text{ m/s} = 6.928 \times 10^8\text{ m/s} \\
v_{pz} &= \frac{\omega}{\beta_z} = \frac{6\pi \times 10^7}{0.1\pi} = 6 \times 10^8\text{ m/s}
\end{aligned}$$

Finally, to verify (8.20) and (8.22), we note that

$$\begin{aligned}
\frac{1}{\lambda_x^2} + \frac{1}{\lambda_y^2} + \frac{1}{\lambda_z^2} &= \frac{1}{(40/3)^2} + \frac{1}{(40/\sqrt{3})^2} + \frac{1}{20^2} \\
&= \frac{9}{1600} + \frac{3}{1600} + \frac{4}{1600} = \frac{1}{100} = \frac{1}{10^2} = \frac{1}{\lambda^2}
\end{aligned}$$

and

$$\begin{aligned}
\frac{1}{v_{px}^2} + \frac{1}{v_{py}^2} + \frac{1}{v_{pz}^2} &= \frac{1}{(4 \times 10^8)^2} + \frac{1}{(4\sqrt{3} \times 10^8)^2} + \frac{1}{(6 \times 10^8)^2} \\
&= \frac{1}{16 \times 10^{16}} + \frac{1}{48 \times 10^{16}} + \frac{1}{36 \times 10^{16}} \\
&= \frac{1}{9 \times 10^{16}} = \frac{1}{(3 \times 10^8)^2} = \frac{1}{v_p^2}
\end{aligned}$$

8.2 TRANSVERSE ELECTRIC WAVES IN A PARALLEL-PLATE WAVEGUIDE

Let us now consider the superposition of two uniform plane waves propagating symmetrically with respect to the z-axis, as shown in Figure 8.4, and having the electric fields

$$\begin{aligned}\mathbf{E}_1 &= E_0 \cos\,(\omega t - \boldsymbol{\beta}_1 \cdot \mathbf{r})\,\mathbf{a}_y \\ &= E_0 \cos\,(\omega t + \beta x \cos\theta - \beta z \sin\theta)\,\mathbf{a}_y \end{aligned} \tag{8.23a}$$

$$\begin{aligned}\mathbf{E}_2 &= -E_0 \cos\,(\omega t - \boldsymbol{\beta}_2 \cdot \mathbf{r})\,\mathbf{a}_y \\ &= -E_0 \cos\,(\omega t - \beta x \cos\theta - \beta z \sin\theta)\,\mathbf{a}_y \end{aligned} \tag{8.23b}$$

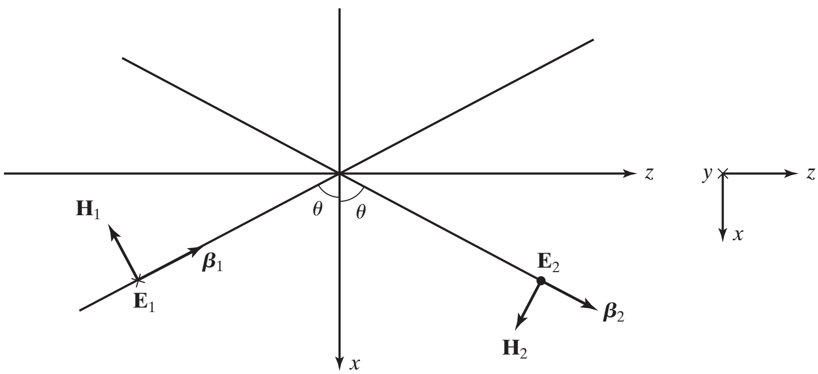

FIGURE 8.4

Superposition of two uniform plane waves propagating symmetrically with respect to the z-axis.

where $\beta = \omega\sqrt{\mu\epsilon}$, with ϵ and μ being the permittivity and the permeability, respectively, of the medium. The corresponding magnetic fields are given by

$$\mathbf{H}_1 = \frac{E_0}{\eta}(-\sin\theta\,\mathbf{a}_x - \cos\theta\,\mathbf{a}_z)\cos(\omega t + \beta x\cos\theta - \beta z\sin\theta) \tag{8.24a}$$

$$\mathbf{H}_2 = \frac{E_0}{\eta}(\sin\theta\,\mathbf{a}_x - \cos\theta\,\mathbf{a}_z)\cos(\omega t - \beta x\cos\theta - \beta z\sin\theta) \tag{8.24b}$$

where $\eta = \sqrt{\mu/\epsilon}$. The electric and magnetic fields of the superposition of the two waves are given by

$$\begin{aligned}\mathbf{E} &= \mathbf{E}_1 + \mathbf{E}_2 \\ &= E_0[\cos\,(\omega t - \beta z\sin\theta + \beta x\cos\theta) \\ &\quad - \cos\,(\omega t - \beta z\sin\theta - \beta x\cos\theta)]\mathbf{a}_y \\ &= -2E_0 \sin\,(\beta x\cos\theta)\,\sin\,(\omega t - \beta z\sin\theta)\,\mathbf{a}_y\end{aligned} \tag{8.25a}$$

$$
\begin{aligned}
\mathbf{H} &= \mathbf{H}_1 + \mathbf{H}_2 \\
&= -\frac{E_0}{\eta} \sin\theta\, [\cos(\omega t - \beta z \sin\theta + \beta x \cos\theta) \\
&\quad - \cos(\omega t - \beta z \sin\theta - \beta x \cos\theta)]\mathbf{a}_x \\
&\quad - \frac{E_0}{\eta} \cos\theta\, [\cos(\omega t - \beta z \sin\theta + \beta x \cos\theta) \\
&\quad + \cos(\omega t - \beta z \sin\theta - \beta x \cos\theta)]\mathbf{a}_z \\
&= \frac{2E_0}{\eta} \sin\theta \sin(\beta x \cos\theta) \sin(\omega t - \beta z \sin\theta)\,\mathbf{a}_x \\
&\quad - \frac{2E_0}{\eta} \cos\theta \cos(\beta x \cos\theta) \cos(\omega t - \beta z \sin\theta)\,\mathbf{a}_z
\end{aligned} \tag{8.25b}
$$

In view of the factors $\sin(\beta x \cos\theta)$ and $\cos(\beta x \cos\theta)$ for the x-dependence and the factors $\sin(\omega t - \beta z \sin\theta)$ and $\cos(\omega t - \beta z \sin\theta)$ for the z-dependence, the composite fields have standing wave character in the x-direction and traveling wave character in the z-direction. Thus, we have standing waves in the x-direction moving bodily in the z-direction, as illustrated in Figure 8.5, by considering the electric field for two different times. In fact, we find that the Poynting vector is given by

$$
\begin{aligned}
\mathbf{P} &= \mathbf{E} \times \mathbf{H} = E_y\mathbf{a}_y \times (H_x\mathbf{a}_x + H_z\mathbf{a}_z) \\
&= -E_yH_x\mathbf{a}_z + E_yH_z\mathbf{a}_x \\
&= \frac{4E_0^2}{\eta} \sin\theta \sin^2(\beta x \cos\theta) \sin^2(\omega t - \beta z \sin\theta)\,\mathbf{a}_z \\
&\quad + \frac{E_0^2}{\eta} \cos\theta \sin(2\beta x \cos\theta) \sin 2(\omega t - \beta z \sin\theta)\,\mathbf{a}_x
\end{aligned} \tag{8.26}
$$

The time-average Poynting vector is given by

$$
\begin{aligned}
\langle \mathbf{P} \rangle &= \frac{4E_0^2}{\eta} \sin\theta \sin^2(\beta x \cos\theta) \langle \sin^2(\omega t - \beta z \sin\theta)\rangle \mathbf{a}_z \\
&\quad + \frac{E_0^2}{\eta} \cos\theta \sin(2\beta x \cos\theta) \langle \sin 2(\omega t - \beta z \sin\theta)\rangle \mathbf{a}_x \\
&= \frac{2E_0^2}{\eta} \sin\theta \sin^2(\beta x \cos\theta)\,\mathbf{a}_z
\end{aligned} \tag{8.27}
$$

Thus, the time-average power flow is entirely in the z-direction, thereby verifying our interpretation of the field expressions. Since the composite electric field is directed entirely transverse to the z-direction, that is, the direction of time-average power flow, whereas the composite magnetic field is not, the composite wave is known as the *transverse electric*, or TE wave.

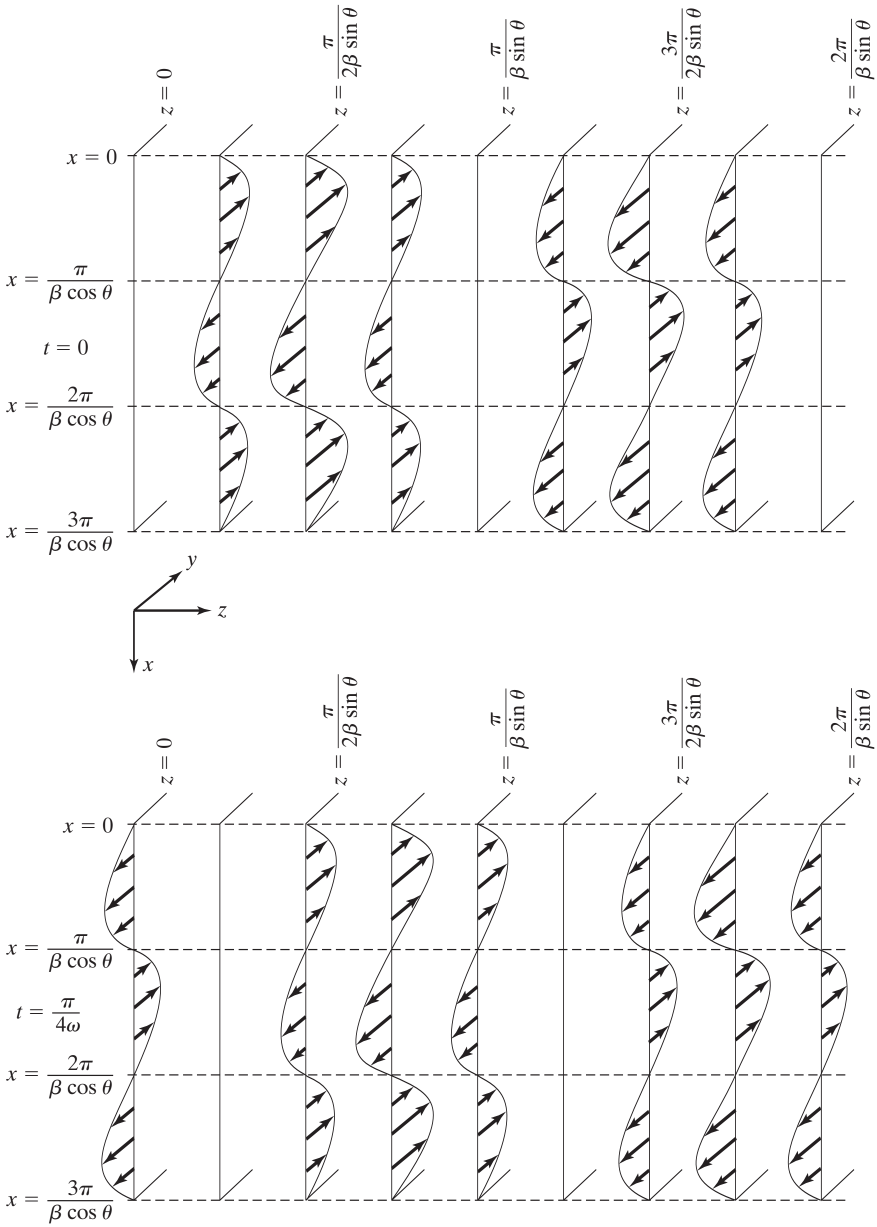

FIGURE 8.5

Standing waves in the x-direction moving bodily in the z-direction.

From the expressions for the fields for the TE wave given by (8.25a) and (8.25b), we note that the electric field is zero for sin $(\beta x \cos\theta)$ equal to zero, or

$$\beta x \cos\theta = \pm m\pi, \qquad m = 0, 1, 2, 3, \ldots$$

$$x = \pm\frac{m\pi}{\beta\cos\theta} = \pm\frac{m\lambda}{2\cos\theta}, \qquad m = 0, 1, 2, 3, \ldots \tag{8.28}$$

where

$$\lambda = \frac{2\pi}{\beta} = \frac{2\pi}{\omega\sqrt{\mu\epsilon}} = \frac{1}{f\sqrt{\mu\epsilon}}$$

Thus, if we place perfectly conducting sheets in these planes, the waves will propagate undisturbed, that is, as though the sheets were not present, since the boundary condition that the tangential component of the electric field be zero on the surface of a perfect conductor is satisfied in these planes. The boundary condition that the normal component of the magnetic field be zero on the surface of a perfect conductor is also satisfied since H_x is zero in these planes.

If we consider any two adjacent sheets, the situation is actually one of uniform plane waves bouncing obliquely between the sheets, as illustrated in Figure 8.6 for two sheets in the planes $x = 0$ and $x = \lambda/(2\cos\theta)$, thereby guiding the wave and hence the energy in the z-direction, parallel to the plates. Thus, we have a *parallel-plate waveguide*, as compared to the parallel-plate transmission line in which the uniform plane wave slides parallel to the plates. We note from the constant phase surfaces of the obliquely bouncing wave shown in Figure 8.6 that $\lambda/(2\cos\theta)$ is simply one-half of the apparent wavelength of that wave in the x-direction, that is, normal to the plates. Thus, the fields have one-half apparent wavelength in the x-direction. If we place the perfectly conducting sheets in the planes $x = 0$ and $x = m\lambda/(2\cos\theta)$, the fields will then have m number of one-half apparent wavelengths in the x-direction between the plates. The fields have no variations in the y-direction. Thus, the fields are said to correspond to $\text{TE}_{m,0}$ *modes*, where the subscript m refers to the x-direction, denoting m number of one-half apparent wavelengths in that direction and the subscript 0 refers to the y-direction, denoting zero number of one-half apparent wavelengths in that direction.

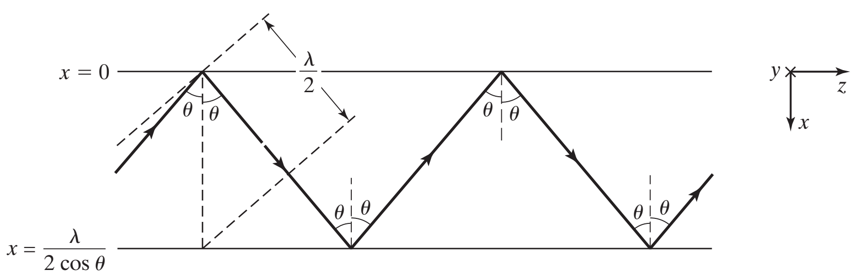

FIGURE 8.6

Uniform plane waves bouncing obliquely between two parallel plane perfectly conducting sheets.

Let us now consider a parallel-plate waveguide with perfectly conducting plates situated in the planes $x = 0$ and $x = a$, that is, having a fixed spacing a between them, as shown in Figure 8.7(a). Then, for $\text{TE}_{m,0}$ waves guided by the plates, we have from (8.28),

$$a = \frac{m\lambda}{2\cos\theta}$$

or

$$\cos\theta = \frac{m\lambda}{2a} = \frac{m}{2a}\frac{1}{f\sqrt{\mu\epsilon}} \tag{8.29}$$

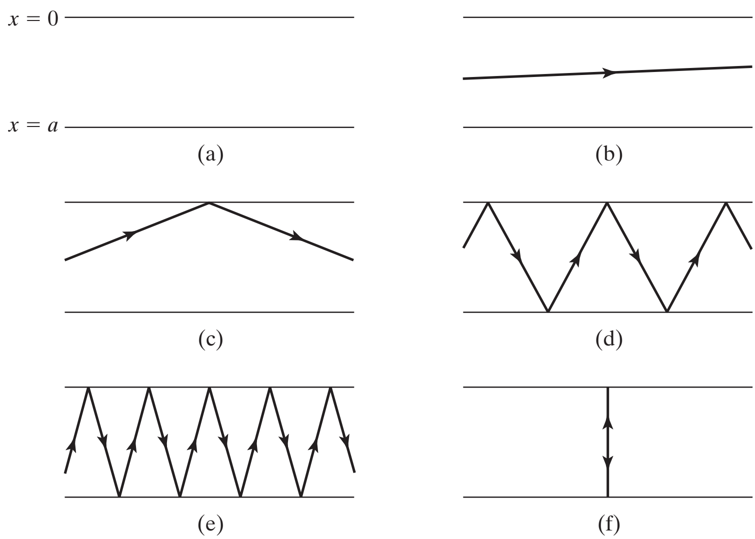

FIGURE 8.7

For illustrating the phenomenon of cutoff in a parallel-plate waveguide.

Thus, waves of different wavelengths (or frequencies) bounce obliquely between the plates at different values of the angle θ. For very small wavelengths (very high frequencies), $m\lambda/2a$ is small, $\cos\theta \approx 0$, $\theta \approx 90°$, and the waves simply slide between the plates as in the case of the transmission line, as shown in Figure 8.7(b). As λ increases (f decreases), $m\lambda/2a$ increases, θ decreases, and the waves bounce more and more obliquely, as shown in Figure 8.7(c)–(e), until λ becomes equal to $2a/m$, for which $\cos\theta = 1$, $\theta = 0°$, and the waves simply bounce back and forth normally to the plates, as shown in Figure 8.7(f), without any feeling of being guided parallel to the plates. For $\lambda > 2a/m$, $m\lambda/2a > 1$, $\cos\theta > 1$, and θ has no real solution, indicating that propagation does not occur for these wavelengths in the waveguide mode. This condition is known as the *cutoff* condition.

The cutoff wavelength, denoted by the symbol λ_c, is given by

$$\lambda_c = \frac{2a}{m} \tag{8.30}$$

This is simply the wavelength for which the spacing a is equal to m number of one-half wavelengths. Propagation of a particular mode is possible only if λ is less than the value of λ_c for that mode. The cutoff frequency is given by

$$f_c = \frac{m}{2a\sqrt{\mu\epsilon}} \tag{8.31}$$

Propagation of a particular mode is possible only if f is greater than the value of f_c for that mode. Consequently, waves of a given frequency f can propagate in all modes for which the cutoff wavelengths are greater than the wavelength or the cutoff frequencies are less than the frequency.

Substituting λ_c for $2a/m$ in (8.29), we have

$$\cos\theta = \frac{\lambda}{\lambda_c} = \frac{f_c}{f} \tag{8.32a}$$

$$\sin\theta = \sqrt{1-\cos^2\theta} = \sqrt{1-\left(\frac{\lambda}{\lambda_c}\right)^2} = \sqrt{1-\left(\frac{f_c}{f}\right)^2} \tag{8.32b}$$

$$\beta\cos\theta = \frac{2\pi}{\lambda}\frac{\lambda}{\lambda_c} = \frac{2\pi}{\lambda_c} = \frac{m\pi}{a} \tag{8.32c}$$

$$\beta\sin\theta = \frac{2\pi}{\lambda}\sqrt{1-\left(\frac{\lambda}{\lambda_c}\right)^2} \tag{8.32d}$$

We see from (8.32d) that the phase constant along the z-direction, that is, $\beta \sin\theta$, is real for $\lambda < \lambda_c$ and imaginary for $\lambda > \lambda_c$, thereby explaining once again the cutoff phenomenon. We now define the guide wavelength, λ_g, to be the wavelength in the z-direction, that is, along the guide. This is given by

$$\lambda_g = \frac{2\pi}{\beta\sin\theta} = \frac{\lambda}{\sqrt{1-(\lambda/\lambda_c)^2}} = \frac{\lambda}{\sqrt{1-(f_c/f)^2}} \tag{8.33}$$

This is simply the apparent wavelength, in the z-direction, of the obliquely bouncing uniform plane waves. The phase velocity along the guide axis, which is simply the apparent phase velocity, in the z-direction, of the obliquely bouncing uniform plane waves, is

$$v_{pz} = \frac{\omega}{\beta\sin\theta} = \frac{v_p}{\sin\theta} = \frac{v_p}{\sqrt{1-(\lambda/\lambda_c)^2}} = \frac{v_p}{\sqrt{1-(f_c/f)^2}} \tag{8.34}$$

We note that the phase velocity along the guide axis is a function of frequency and hence the propagation along the guide axis is characterized by *dispersion*. The topic of dispersion is discussed in the next section.

Finally, substituting (8.32a)–(8.32d) in the field expressions (8.25a) and (8.25b), we obtain

$$\mathbf{E} = -2E_0 \sin\left(\frac{m\pi x}{a}\right)\sin\left(\omega t - \frac{2\pi}{\lambda_g}z\right)\mathbf{a}_y \tag{8.35a}$$

$$\begin{aligned}\mathbf{H} = {} & \frac{2E_0}{\eta}\frac{\lambda}{\lambda_g}\sin\left(\frac{m\pi x}{a}\right)\sin\left(\omega t - \frac{2\pi}{\lambda_g}z\right)\mathbf{a}_x \\ & - \frac{2E_0}{\eta}\frac{\lambda}{\lambda_c}\cos\left(\frac{m\pi x}{a}\right)\cos\left(\omega t - \frac{2\pi}{\lambda_g}z\right)\mathbf{a}_z\end{aligned} \tag{8.35b}$$

These expressions for the $\text{TE}_{m,0}$ mode fields in the parallel-plate waveguide do not contain the angle θ. They clearly indicate the standing wave character of the fields in the x-direction, having m one-half sinusoidal variations between the plates. We shall now consider an example.

Example 8.2

Let us assume the spacing a between the plates of a parallel-plate waveguide to be 5 cm and investigate the propagating $\text{TE}_{m,0}$ modes for $f = 10{,}000$ MHz.

From (8.30), the cutoff wavelengths for $\text{TE}_{m,0}$ modes are given by

$$\lambda_c = \frac{2a}{m} = \frac{10}{m}\text{ cm} = \frac{0.1}{m}\text{ m}$$

This result is independent of the dielectric between the plates. If the medium between the plates is free space, then the cutoff frequencies for the $\text{TE}_{m,0}$ modes are

$$f_c = \frac{3 \times 10^8}{\lambda_c} = \frac{3 \times 10^8}{0.1/m} = 3m \times 10^9 \text{ Hz}$$

For $f = 10{,}000\text{ MHz} = 10^{10}$ Hz, the propagating modes are $\text{TE}_{1,0}(f_c = 3 \times 10^9 \text{ Hz})$, $\text{TE}_{2,0}(f_c = 6 \times 10^9 \text{ Hz})$, and $\text{TE}_{3,0}(f_c = 9 \times 10^9 \text{ Hz})$.

For each propagating mode, we can find θ, λ_g, and v_{pz} by using (8.32a), (8.33), and (8.34), respectively. Values of these quantities are listed in the following:

Mode	λ_c, cm	f_c, MHz	θ, deg	λ_g, cm	v_{pz}, m/s
$\text{TE}_{1,0}$	10	3000	72.54	3.145	3.145×10^8
$\text{TE}_{2,0}$	5	6000	53.13	3.75	3.75×10^8
$\text{TE}_{3,0}$	3.33	9000	25.84	6.882	6.882×10^8

8.3 DISPERSION AND GROUP VELOCITY

In Section 8.2, we learned that for the propagating range of frequencies, the phase velocity and the wavelength along the axis of the parallel-plate waveguide are given by

$$v_{pz} = \frac{v_p}{\sqrt{1 - (f_c/f)^2}} \tag{8.36}$$

and

$$\lambda_g = \frac{\lambda}{\sqrt{1 - (f_c/f)^2}} \tag{8.37}$$

where $v_p = 1/\sqrt{\mu\epsilon}$, $\lambda = v_p/f = 1/f\sqrt{\mu\epsilon}$, and f_c is the cutoff frequency. We note that for a particular mode, the phase velocity of propagation along the guide axis varies with the frequency. As a consequence of this characteristic of the guided wave propagation, the field patterns of the different frequency components of a signal comprising a band of frequencies do not maintain the same phase relationships as they propagate down the guide. This phenomenon is known as *dispersion*, so termed after the phenomenon of dispersion of colors by a prism.

To discuss dispersion, let us consider a simple example of two infinitely long trains A and B traveling in parallel, one below the other, with each train made up of boxcars of identical size and having wavy tops, as shown in Figure 8.8. Let the spacings between the peaks (centers) of successive boxcars be 50 m and 90 m, and let the speeds

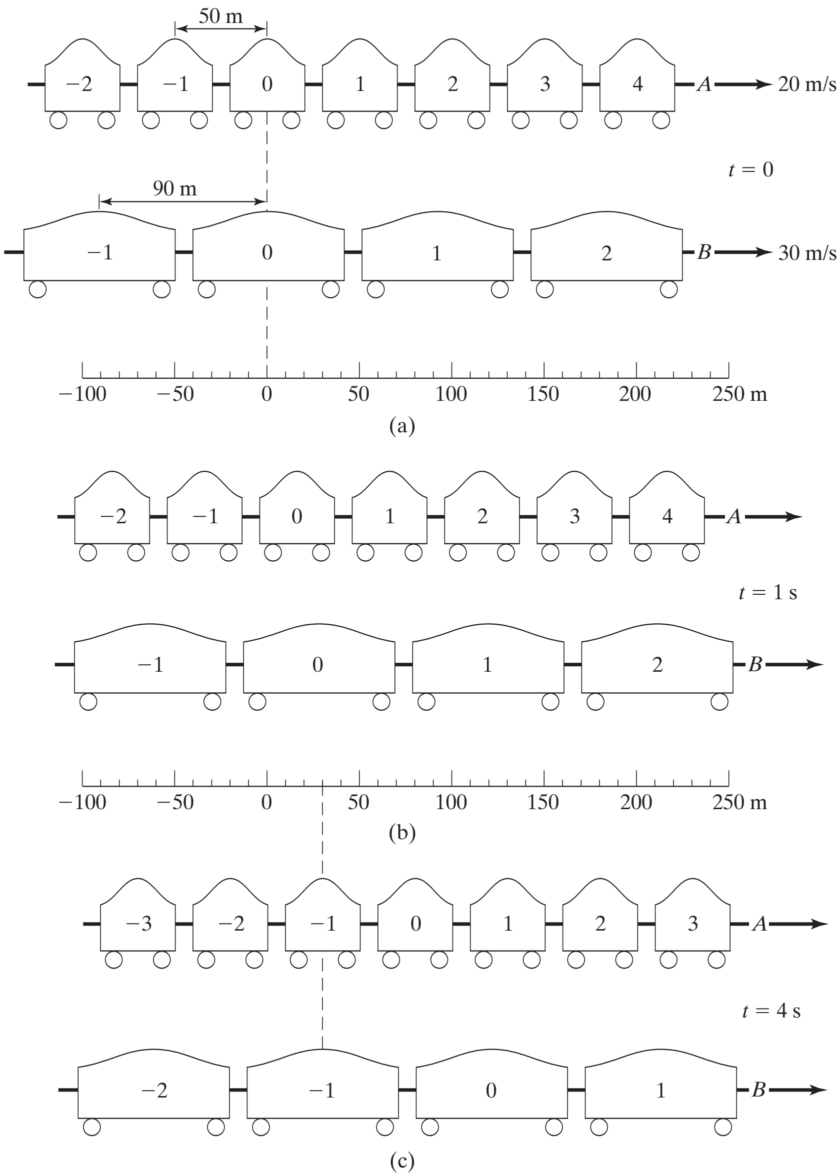

FIGURE 8.8

For illustrating the concept of group velocity.

of the trains be 20 m/s and 30 m/s, for trains A and B, respectively. Let the peaks of the cars numbered 0 for the two trains be aligned at time $t = 0$, as shown in Figure 8.8(a). Now, as time progresses, the two peaks get out of alignment as shown, for example, for $t = 1$ s in Figure 8.8(b), since train B is traveling faster than train A. But at the same time, the gap between the peaks of cars numbered -1 decreases. This continues until at

$t = 4$ s, the peak of car "-1" of train A having moved by a distance of 80 m aligns with the peak of car "-1" of train B, which will have moved by a distance of 120 m, as shown in Figure 8.8(c). For an observer following the movement of the two trains as a group, the group appears to have moved by a distance of 30 m although the individual trains will have moved by 80 m and 120 m, respectively. Thus, we can talk of a *group velocity*, that is, the velocity with which the group as a whole is moving. In this case, the group velocity is 30 m/4 s or 7.5 m/s.

The situation in the case of the guided wave propagation of two different frequencies in the parallel-plate waveguide is exactly similar to the two-train example just discussed. The distance between the peaks of two successive cars is analogous to the guide wavelength, and the speed of the train is analogous to the phase velocity along the guide axis. Thus, let us consider the field patterns corresponding to two waves of frequencies f_A and f_B propagating in the same mode, having guide wavelengths λ_{gA} and λ_{gB}, and phase velocities along the guide axis v_{pzA} and v_{pzB}, respectively, as shown, for example, for the electric field of the $\text{TE}_{1,0}$ mode in Figure 8.9. Let the positive peaks numbered 0 of the two patterns be aligned $t = 0$, as shown in Figure 8.9(a). As the individual waves travel with their respective phase velocities along the guide, these two peaks get out of alignment but some time later, say Δt, the positive peaks numbered -1 will align at some distance, say Δz, from the location of the alignment of the "0" peaks, as shown in Figure 8.9(b). Since the "-1"th peak of wave A will have traveled a distance $\lambda_{gA} + \Delta z$ with a phase velocity v_{pzA} and the "-1"th peak of wave B will have traveled a distance $\lambda_{gB} + \Delta z$ with a phase velocity v_{pzB} in this time Δt, we have

$$\lambda_{gA} + \Delta z = v_{pzA}\,\Delta t \tag{8.38a}$$

$$\lambda_{gB} + \Delta z = v_{pzB}\,\Delta t \tag{8.38b}$$

Solving (8.38a) and (8.38b) for Δt and Δz, we obtain

$$\Delta t = \frac{\lambda_{gA} - \lambda_{gB}}{v_{pzA} - v_{pzB}} \tag{8.39a}$$

and

$$\Delta z = \frac{\lambda_{gA} v_{pzB} - \lambda_{gB} v_{pzA}}{v_{pzA} - v_{pzB}} \tag{8.39b}$$

The group velocity, v_g, is then given by

$$\begin{aligned} v_g &= \frac{\Delta z}{\Delta t} = \frac{\lambda_{gA} v_{pzB} - \lambda_{gB} v_{pzA}}{\lambda_{gA} - \lambda_{gB}} = \frac{\lambda_{gA}\lambda_{gB} f_B - \lambda_{gB}\lambda_{gA} f_A}{\lambda_{gA}\lambda_{gB}\left(\dfrac{1}{\lambda_{gB}} - \dfrac{1}{\lambda_{gA}}\right)} \\ &= \frac{f_B - f_A}{\dfrac{1}{\lambda_{gB}} - \dfrac{1}{\lambda_{gA}}} = \frac{\omega_B - \omega_A}{\beta_{zB} - \beta_{zA}} \end{aligned} \tag{8.40}$$

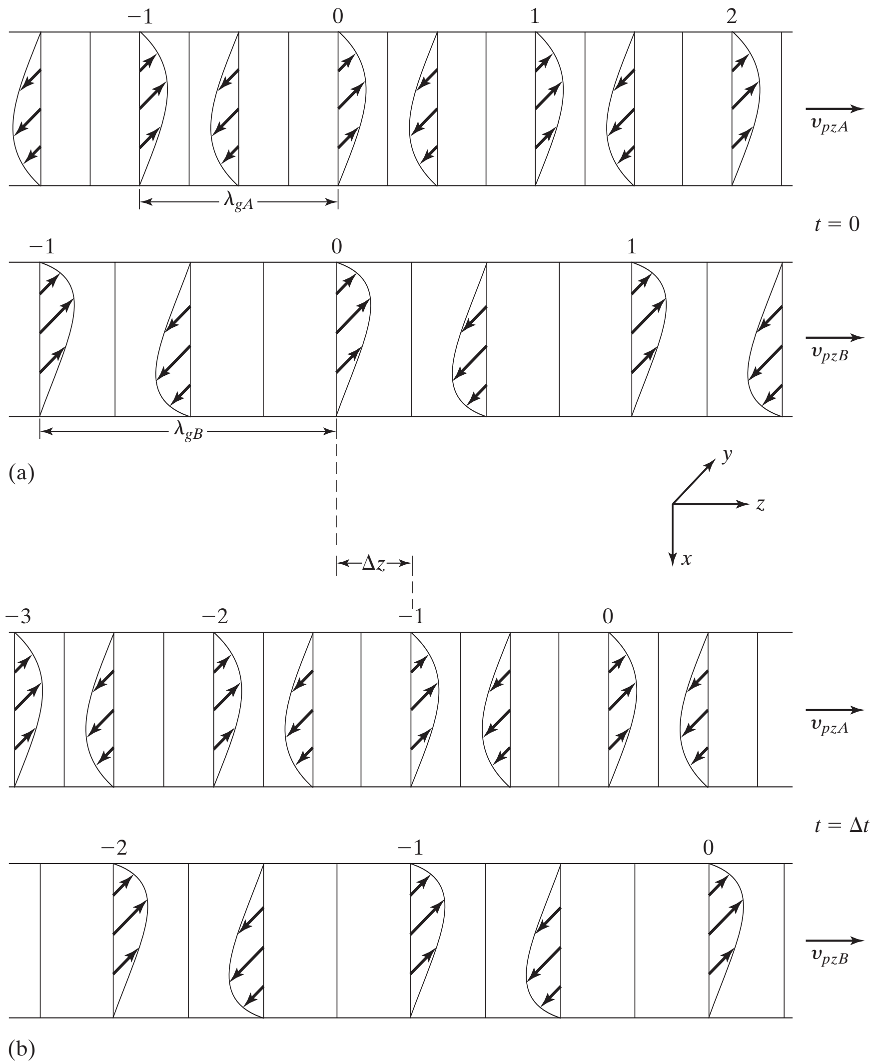

FIGURE 8.9

For illustrating the concept of group velocity for guided wave propagation.

where β_{zA} and β_{zB} are the phase constants along the guide axis, corresponding to f_A and f_B, respectively. Thus, the group velocity of a signal comprised of two frequencies is the ratio of the difference between the two radian frequencies to the difference between the corresponding phase constants along the guide axis.

If we now have a signal comprised of a number of frequencies, then a value of group velocity can be obtained for each pair of these frequencies in accordance with (8.40). In general, these values of group velocity will all be different. In fact, this is the case for wave propagation in the parallel-plate guide, as can be seen from Figure 8.10, which is a plot of ω versus β_z corresponding to the parallel-plate guide for which

$$\beta_z = \frac{2\pi}{\lambda_g} = \frac{2\pi}{\lambda}\sqrt{1 - \left(\frac{\lambda}{\lambda_c}\right)^2} = \omega\sqrt{\mu\epsilon}\sqrt{1 - \left(\frac{f_c}{f}\right)^2} \tag{8.41}$$

Such a plot is known as the *ω–β_z diagram* or the *dispersion diagram.*

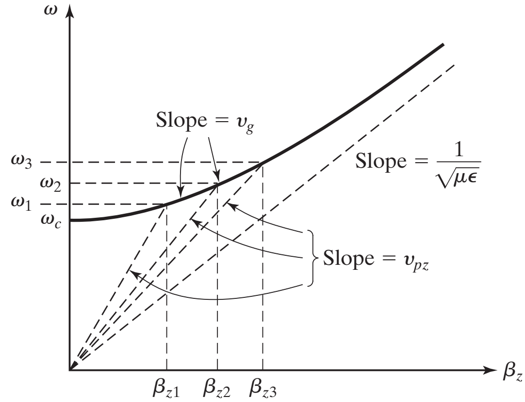

FIGURE 8.10

Dispersion diagram for the parallel-plate waveguide.

The phase velocity, ω/β_z, for a particular frequency is given by the slope of the line drawn from the origin to the point, on the dispersion curve, corresponding to that frequency, as shown in the figure for the three frequencies ω_1, ω_2, and ω_3. The group velocity for a particular pair of frequencies is given by the slope of the line joining the two points, on the curve, corresponding to the two frequencies, as shown in the figure for the two pairs ω_1, ω_2 and ω_2, ω_3. Since the curve is nonlinear, it can be seen that the two group velocities are not equal. We cannot then attribute a particular value of group velocity for the group of the three frequencies ω_1, ω_2, and ω_3.

If, however, the three frequencies are very close, as in the case of a narrow-band signal, it is meaningful to assign a group velocity to the entire group having a value equal to the slope of the tangent to the dispersion curve at the center frequency. Thus, the group velocity corresponding to a narrow band of frequencies centered around a predominant frequency ω is given by

$$v_g = \frac{d\omega}{d\beta_z} \tag{8.42}$$

For the parallel-plate waveguide under consideration, we have from (8.41),

$$\begin{aligned}
\frac{d\beta_z}{d\omega} &= \sqrt{\mu\epsilon}\sqrt{1 - \left(\frac{f_c}{f}\right)^2} + \omega\sqrt{\mu\epsilon}\cdot\frac{1}{2}\left(1 - \frac{f_c^2}{f^2}\right)^{-1/2}\frac{f_c^2}{\pi f^3} \\
&= \sqrt{\mu\epsilon}\left(1 - \frac{f_c^2}{f^2} + \frac{\omega}{2\pi}\frac{f_c^2}{f^3}\right)\left(1 - \frac{f_c^2}{f^2}\right)^{-1/2} \\
&= \sqrt{\mu\epsilon}\left(1 - \frac{f_c^2}{f^2}\right)^{-1/2}
\end{aligned}$$

and

$$v_g = \frac{d\omega}{d\beta_z} = \frac{1}{\sqrt{\mu\epsilon}}\sqrt{1 - \frac{f_c^2}{f^2}} = v_p\sqrt{1 - \left(\frac{f_c}{f}\right)^2} \tag{8.43}$$

As a numerical example, for the case of Example 8.2, the group velocities for $f = 10{,}000$ MHz for the three propagating modes $\mathrm{TE}_{1,0}$, $\mathrm{TE}_{2,0}$, and $\mathrm{TE}_{3,0}$ are 2.862×10^8 m/s, 2.40×10^8 m/s, and 1.308×10^8 m/s, respectively. From (8.36) and (8.43), we note that

$$v_{pz}v_g = v_p^2 \tag{8.44}$$

An example of a narrow-band signal is an amplitude modulated signal, having a carrier frequency ω modulated by a low frequency $\Delta\omega \ll \omega$, as given by

$$E_x(t) = E_{x0}(1 + m\cos\Delta\omega \cdot t)\cos\omega t \tag{8.45}$$

where m is the percentage modulation. Such a signal is actually equivalent to a superposition of unmodulated signals of three frequencies $\omega - \Delta\omega$, ω, and $\omega + \Delta\omega$, as can be seen by expanding the right side of (8.45). Thus

$$\begin{aligned} E_x(t) &= E_{x0}\cos\omega t + mE_{x0}\cos\omega t\cos\Delta\omega \cdot t \\ &= E_{x0}\cos\omega t + \frac{mE_{x0}}{2}[\cos(\omega - \Delta\omega)t + \cos(\omega + \Delta\omega)t] \end{aligned} \tag{8.46}$$

The frequencies $\omega - \Delta\omega$ and $\omega + \Delta\omega$ are the side frequencies. When the amplitude modulated signal propagates in a dispersive channel such as the parallel-plate waveguide under consideration, the different frequency components undergo phase changes in accordance with their respective phase constants. Thus, if $\beta_z - \Delta\beta_z$, β_z, and $\beta_z + \Delta\beta_z$ are the phase constants corresponding to $\omega - \Delta\omega$, ω, and $\omega + \Delta\omega$, respectively, assuming linearity of the dispersion curve within the narrow band, the amplitude modulated wave is given by

$$\begin{aligned} E_x(z,t) &= E_{x0}\cos(\omega t - \beta_z z) \\ &\quad + \frac{mE_{x0}}{2}\{\cos[(\omega - \Delta\omega)t - (\beta_z - \Delta\beta_z)z] \\ &\quad + \cos[(\omega + \Delta\omega)t - (\beta_z + \Delta\beta_z)z]\} \\ &= E_{x0}\cos(\omega t - \beta_z z) \\ &\quad + \frac{mE_{x0}}{2}\{\cos[(\omega t - \beta_z z) - (\Delta\omega \cdot t - \Delta\beta_z \cdot z)] \\ &\quad + \cos[(\omega t - \beta_z z) + (\Delta\omega \cdot t - \Delta\beta_z \cdot z)]\} \\ &= E_{x0}\cos(\omega t - \beta_z z) + mE_{x0}\cos(\omega t - \beta_z z)\cos(\Delta\omega \cdot t - \Delta\beta_z \cdot z) \\ &= E_{x0}[1 + m\cos(\Delta\omega \cdot t - \Delta\beta_z \cdot z)]\cos(\omega t - \beta_z z) \end{aligned} \tag{8.47}$$

This indicates that although the carrier frequency phase changes in accordance with the phase constant β_z, the modulation envelope and hence the information travels with the group velocity $\Delta\omega/\Delta\beta_z$, as shown in Figure 8.11. In view of this and since v_g is less than v_p, the fact that v_{pz} is greater than v_p is not a violation of the theory of relativity. Since it is always necessary to use some modulation technique to convey information from one point to another, the information always takes more time to reach from one point to another in a dispersive channel than in the corresponding nondispersive medium.

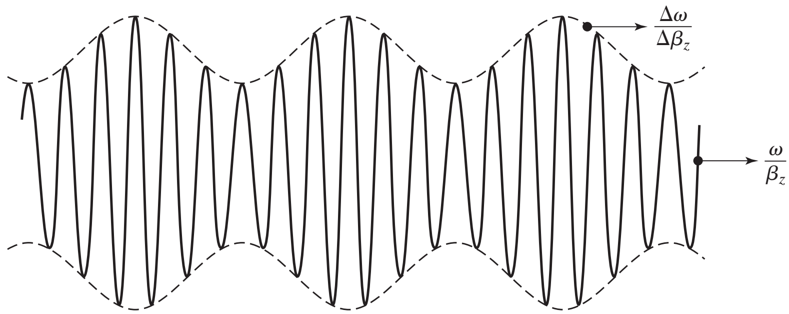

FIGURE 8.11

For illustrating that the modulation envelope travels with the group velocity.

8.4 RECTANGULAR WAVEGUIDE AND CAVITY RESONATOR

Thus far, we have restricted our discussion to $\text{TE}_{m,0}$ wave propagation in a parallel-plate waveguide. From Section 8.2, we recall that the parallel-plate waveguide is made up of two perfectly conducting sheets in the planes $x = 0$ and $x = a$ and that the electric field of the $\text{TE}_{m,0}$ mode has only a y-component with m number of one-half sinusoidal variations in the x-direction and no variations in the y-direction. If we now introduce two perfectly conducting sheets in two constant y-planes, say, $y = 0$ and $y = b$, the field distribution will remain unaltered, since the electric field is entirely normal to the plates, and hence the boundary condition of zero tangential electric field is satisfied for both sheets. We then have a metallic pipe with rectangular cross section in the xy-plane, as shown in Figure 8.12. Such a structure is known as the *rectangular waveguide* and is, in fact, a common form of waveguide.

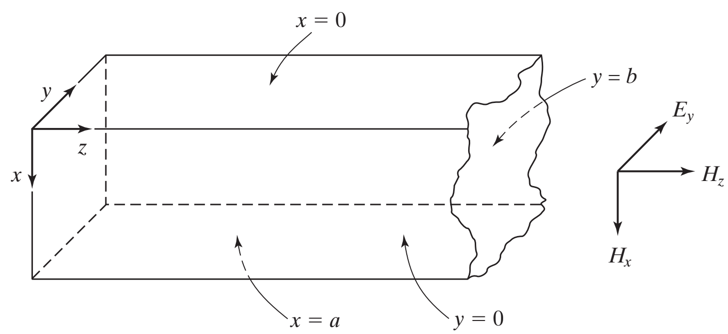

FIGURE 8.12

A rectangular waveguide.

Since the $TE_{m,0}$ mode field expressions derived for the parallel-plate waveguide satisfy the boundary conditions for the rectangular waveguide, those expressions as well as the entire discussion of the parallel-plate waveguide case hold also for $TE_{m,0}$ mode propagation in the rectangular waveguide case. We learned that the $TE_{m,0}$ modes can be interpreted as due to uniform plane waves having electric field in the y-direction and bouncing obliquely between the conducting walls $x = 0$ and $x = a$, and with the associated cutoff condition characterized by bouncing of the waves back and forth normally to these walls, as shown in Figure 8.13(a). For the cutoff condition, the dimension a is equal to m number of one-half wavelengths such that

$$[\lambda_c]_{TE_{m,0}} = \frac{2a}{m} \tag{8.48}$$

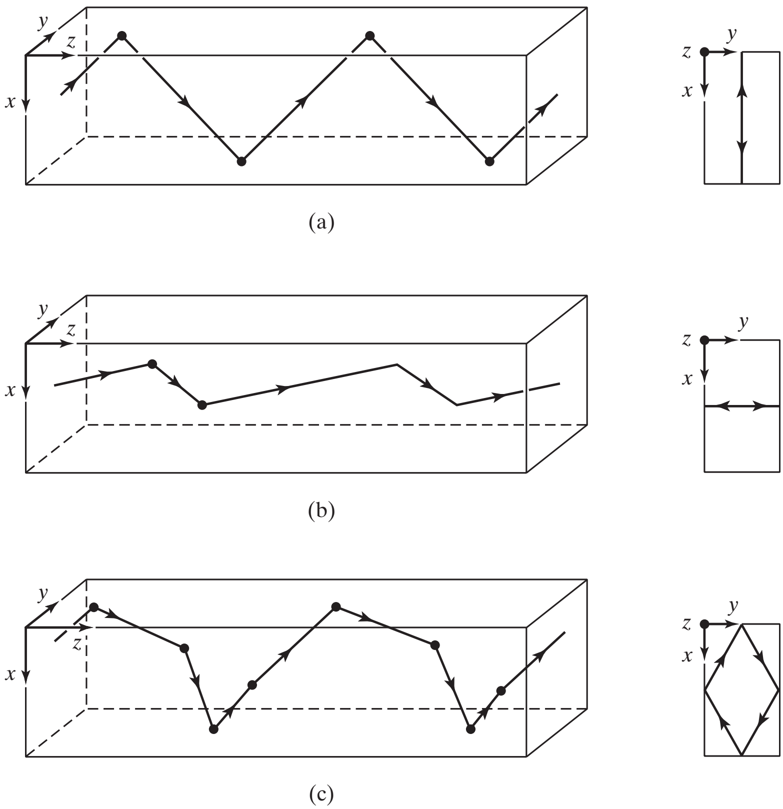

FIGURE 8.13

Propagation and cutoff of (a) $TE_{m,0}$, (b) $TE_{0,n}$, and (c) $TE_{m,n}$ modes in a rectangular waveguide.

In a similar manner, we can have uniform plane waves having electric field in the x-direction and bouncing obliquely between the walls $y = 0$ and $y = b$, and with the associated cutoff condition characterized by bouncing of the waves back and forth normally to these walls, as shown in Figure 8.13(b), thereby resulting in $TE_{0,n}$ modes having no variations in the x-direction and n number of one-half sinusoidal variations in the y-direction. For the cutoff condition, the dimension b is equal to n number of one-half wavelengths such that

$$[\lambda_c]_{\mathrm{TE}_{0,n}} = \frac{2b}{n} \tag{8.49}$$

We can even have $\mathrm{TE}_{m,n}$ modes having m number of one-half sinusoidal variations in the x-direction and n number of one-half sinusoidal variations in the y-direction due to uniform plane waves having both x- and y-components of the electric field and bouncing obliquely between all four walls of the guide and with the associated cutoff condition characterized by bouncing of the waves back and forth obliquely between the four walls as shown, for example, in Figure 8.13(c). For the cutoff condition, the dimension a must be equal to m number of one-half apparent wavelengths in the x-direction and the dimension b must be equal to n number of one-half apparent wavelengths in the y-direction such that

$$\frac{1}{[\lambda_c]^2_{\mathrm{TE}_{m,n}}} = \frac{1}{(2a/m)^2} + \frac{1}{(2b/n)^2} \tag{8.50}$$

or

$$[\lambda_c]_{\mathrm{TE}_{m,n}} = \frac{1}{\sqrt{(m/2a)^2 + (n/2b)^2}} \tag{8.51}$$

The entire treatment of guided waves in Section 8.2 can be repeated starting with the superposition of two uniform plane waves having their magnetic fields entirely in the y-direction, thereby leading to *transverse magnetic waves*, or *TM waves*, so termed because the magnetic field for these waves has no z-component, whereas the electric field has. Insofar as the cutoff phenomenon is concerned, these modes are obviously governed by the same condition as the corresponding TE modes. There cannot, however, be any $\mathrm{TM}_{m,0}$ or $\mathrm{TM}_{0,n}$ modes in a rectangular waveguide, since the z-component of the electric field, being tangential to all four walls of the guide, requires sinusoidal variations in both x- and y-directions in order that the boundary condition of zero tangential component of electric field is satisfied on all four walls. Thus, for $\mathrm{TM}_{m,n}$ modes in a rectangular waveguide, both m and n must be nonzero and the cutoff wavelengths are the same as for the $\mathrm{TE}_{m,n}$ modes, that is,

$$[\lambda_c]_{\mathrm{TM}_{m,n}} = \frac{1}{\sqrt{(m/2a)^2 + (n/2b)^2}} \tag{8.52}$$

The foregoing discussion of the modes of propagation in a rectangular waveguide points out that a signal of given frequency can propagate in several modes, namely, all modes for which the cutoff frequencies are less than the signal frequency or the cutoff wavelengths are greater than the signal wavelength. Waveguides are, however, designed so that only one mode, the mode with the lowest cutoff frequency (or the largest cutoff wavelength), propagates. This is known as the *dominant mode.* From (8.48), (8.49), (8.51), and (8.52), we can see that the dominant mode is the $\mathrm{TE}_{1,0}$ mode or the $\mathrm{TE}_{0,1}$ mode, depending on whether the dimension a or the dimension b is the larger of the two. By convention, the larger dimension is designated to be a, and hence the $\mathrm{TE}_{1,0}$ mode is the dominant mode. We shall now consider an example.

Example 8.3

It is desired to determine the lowest four cutoff frequencies referred to the cutoff frequency of the dominant mode for three cases of rectangular waveguide dimensions: (i) $b/a = 1$, (ii) $b/a = 1/2$, and (iii) $b/a = 1/3$. Given $a = 3$ cm, it is then desired to find the propagating mode(s) for $f = 9000$ MHz for each of the three cases.

From (8.51) and (8.52), the expression for the cutoff wavelength for a $\text{TE}_{m,n}$ mode where $m = 0, 1, 2, 3, \ldots$ and $n = 0, 1, 2, 3, \ldots$ but not both m and n equal to zero and for a $\text{TM}_{m,n}$ mode where $m = 1, 2, 3, \ldots$ and $n = 1, 2, 3, \ldots$ is given by

$$\lambda_c = \frac{1}{\sqrt{(m/2a)^2 + (n/2b)^2}}$$

The corresponding expression for the cutoff frequency is

$$\begin{aligned} f_c = \frac{v_p}{\lambda_c} &= \frac{1}{\sqrt{\mu\epsilon}}\sqrt{\left(\frac{m}{2a}\right)^2 + \left(\frac{n}{2b}\right)^2} \\ &= \frac{1}{2a\sqrt{\mu\epsilon}}\sqrt{m^2 + \left(n\frac{a}{b}\right)^2} \end{aligned}$$

The cutoff frequency of the dominant mode $\text{TE}_{1,0}$ is $1/2a\sqrt{\mu\epsilon}$. Hence,

$$\frac{f_c}{[f_c]_{\text{TE}_{1,0}}} = \sqrt{m^2 + \left(n\frac{a}{b}\right)^2}$$

By assigning different pairs of values for m and n, the lowest four values of $f_c/[f_c]_{\text{TE}_{1,0}}$ can be computed for each of the three specified values of b/a. These computed values and the corresponding modes are shown in Figure 8.14.

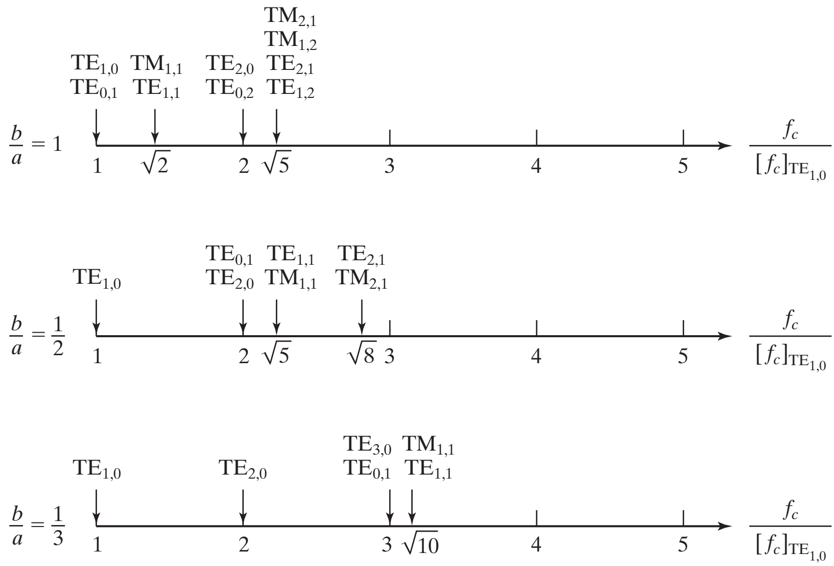

FIGURE 8.14

Lowest four cutoff frequencies referred to the cutoff frequency of the dominant mode for three cases of rectangular waveguide dimensions.

For $a = 3$ cm, and assuming free space for the dielectric in the waveguide,

$$[f_c]_{\mathrm{TE}_{1,0}} = \frac{1}{2a\sqrt{\mu\epsilon}} = \frac{3 \times 10^8}{2 \times 0.03} = 5000\ \mathrm{MHz}$$

Hence, for a signal of frequency $f = 9000$ MHz, all the modes for which $f_c/[f_c]_{\mathrm{TE}_{1,0}}$ is less than 1.8 propagate. From Figure 8.14, these are

$$\begin{array}{ll} \mathrm{TE}_{1,0}, \mathrm{TE}_{0,1}, \mathrm{TM}_{1,1}, \mathrm{TE}_{1,1} & \text{for } b/a = 1 \\ \mathrm{TE}_{1,0} & \text{for } b/a = 1/2 \\ \mathrm{TE}_{1,0} & \text{for } b/a = 1/3 \end{array}$$

It can be seen from Figure 8.14 that for $b/a \leq 1/2$, the second lowest cutoff frequency that corresponds to that of the $\mathrm{TE}_{2,0}$ mode is twice the cutoff frequency of the dominant mode $\mathrm{TE}_{1,0}$. For this reason, the dimension b of a rectangular waveguide is generally chosen to be less than or equal to $a/2$ in order to achieve single-mode transmission over a complete octave (factor of two) range of frequencies.

Let us now consider guided waves of equal magnitude propagating in the positive z- and negative z-directions in a rectangular waveguide. This can be achieved by terminating the guide by a perfectly conducting sheet in a constant-z plane, that is, a transverse plane of the guide. Due to perfect reflection from the sheet, the fields will then be characterized by standing wave nature along the guide axis, that is, in the z-direction, in addition to the standing wave nature in the x- and y-directions. The standing wave pattern along the guide axis will have nulls of transverse electric field on the terminating sheet and in planes parallel to it at distances of integer multiples of $\lambda_g/2$ from that sheet. Placing of perfect conductors in these planes will not disturb the fields, since the boundary condition of zero tangential electric field is satisfied in those planes.

Conversely, if we place two perfectly conducting sheets in two constant-z planes separated by a distance d, then, in order for the boundary conditions to be satisfied, d must be equal to an integer multiple of $\lambda_g/2$. We then have a rectangular box of dimensions a, b, and d in the x-, y-, and z-directions, respectively, as shown in Figure 8.15. Such a structure is known as a *cavity resonator* and is the counterpart of the low-frequency lumped parameter resonant circuit at microwave frequencies since it supports

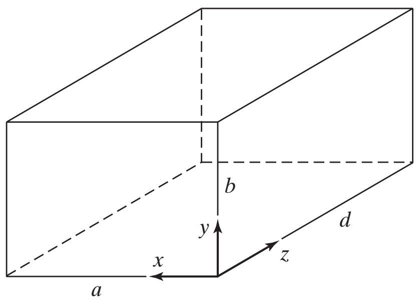

FIGURE 8.15

A rectangular cavity resonator.

oscillations at frequencies for which the above condition, that is,

$$d = l\frac{\lambda_g}{2}, \qquad l = 1, 2, 3, \ldots \tag{8.53}$$

is satisfied. Recalling that λ_g is simply the apparent wavelength of the obliquely bouncing uniform plane wave along the z-direction, we find that the wavelength corresponding to the mode of oscillation for which the fields have m number of one-half sinusoidal variations in the x-direction, n number of one-half sinusoidal variations in the y-direction, and l number of one-half sinusoidal variations in the z-direction is given by

$$\frac{1}{\lambda_{\text{osc}}^2} = \frac{1}{(2a/m)^2} + \frac{1}{(2b/n)^2} + \frac{1}{(2d/l)^2} \tag{8.54}$$

or

$$\lambda_{\text{osc}} = \frac{1}{\sqrt{(m/2a)^2 + (n/2b)^2 + (l/2d)^2}} \tag{8.55}$$

The expression for the frequency of oscillation is then given by

$$f_{\text{osc}} = \frac{v_p}{\lambda_{\text{osc}}} = \frac{1}{\sqrt{\mu\epsilon}}\sqrt{\left(\frac{m}{2a}\right)^2 + \left(\frac{n}{2b}\right)^2 + \left(\frac{l}{2d}\right)^2} \tag{8.56}$$

The modes are designated by three subscripts in the manner $\text{TE}_{m,n,l}$ and $\text{TM}_{m,n,l}$. Since m, n, and l can assume combinations of integer values, an infinite number of frequencies of oscillation are possible for a given set of dimensions for the cavity resonator. We shall now consider an example.

Example 8.4

The dimensions of a rectangular cavity resonator with air dielectric are $a = 4$ cm, $b = 2$ cm, and $d = 4$ cm. It is desired to determine the three lowest frequencies of oscillation and specify the mode(s) of oscillation, transverse with respect to the z-direction, for each frequency.

By substituting $\mu = \mu_0$, $\epsilon = \epsilon_0$, and the given dimensions for a, b, and d in (8.56), we obtain

$$\begin{aligned} f_{\text{osc}} &= 3 \times 10^8\sqrt{\left(\frac{m}{0.08}\right)^2 + \left(\frac{n}{0.04}\right)^2 + \left(\frac{l}{0.08}\right)^2} \\ &= 3750\sqrt{m^2 + 4n^2 + l^2}\ \text{MHz} \end{aligned}$$

By assigning combinations of integer values for m, n, and l and recalling that both m and n must be nonzero for TM modes, we obtain the three lowest frequencies of oscillation to be

$3750 \times \sqrt{2} = 5303$ MHz for $\text{TE}_{1,0,1}$ mode

$3750 \times \sqrt{5} = 8385$ MHz for $\text{TE}_{0,1,1}$, $\text{TE}_{2,0,1}$, and $\text{TE}_{1,0,2}$ modes

$3750 \times \sqrt{6} = 9186$ MHz for $\text{TE}_{1,1,1}$ and $\text{TM}_{1,1,1}$ modes

8.5 REFLECTION AND REFRACTION OF PLANE WAVES

Let us now consider a uniform plane wave that is incident obliquely on a plane boundary between two different perfect dielectric media at an angle of incidence θ_i to the normal to the boundary, as shown in Figure 8.16. To satisfy the boundary conditions at the interface between the two media, a reflected wave and a transmitted wave will be set up. Let θ_r be the angle of reflection and θ_t be the angle of transmission. Then without writing the expressions for the fields, we can find the relationship among θ_i, θ_r, and θ_t by noting that for the incident, reflected, and transmitted waves to be in step at the boundary, their apparent phase velocities parallel to the boundary must be equal; that is,

$$\frac{v_{p1}}{\sin\theta_i} = \frac{v_{p1}}{\sin\theta_r} = \frac{v_{p2}}{\sin\theta_t} \tag{8.57}$$

where $v_{p1}(= 1/\sqrt{\mu_1\epsilon_1})$ and $v_{p2}(= 1/\sqrt{\mu_2\epsilon_2})$ are the phase velocities along the directions of propagation of the waves in medium 1 and medium 2, respectively.

From (8.57), we have

$$\sin\theta_r = \sin\theta_i \tag{8.58}$$

$$\sin\theta_t = \frac{v_{p2}}{v_{p1}}\sin\theta_i = \sqrt{\frac{\mu_1\epsilon_1}{\mu_2\epsilon_2}}\sin\theta_i \tag{8.59}$$

or

$$\theta_r = \theta_i \tag{8.60}$$

$$\theta_t = \sin^{-1}\left(\sqrt{\frac{\mu_1\epsilon_1}{\mu_2\epsilon_2}}\sin\theta_i\right) \tag{8.61}$$

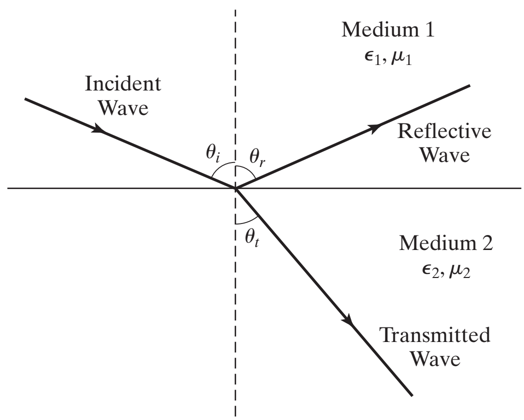

FIGURE 8.16

Reflection and transmission of an obliquely incident uniform plane wave on a plane boundary between two different perfect dielectric media.

Equation (8.60) is known as the *law of reflection* and (8.61) is known as the *law of refraction*, or *Snell's law.* Snell's law is commonly cast in terms of the refractive index, denoted by the symbol n and defined as the ratio of the velocity of light in free space to the phase velocity in the medium. Thus, if $n_1(= c/v_{p1})$ and $n_2(= c/v_{p2})$ are the (phase) refractive indices for media 1 and 2, respectively, then

$$\theta_t = \sin^{-1}\left(\frac{n_1}{n_2}\sin\theta_i\right) \tag{8.62}$$

For two dielectrics having $\mu_1 = \mu_2 = \mu_0$, which is usually the case, (8.62) reduces to

$$\theta_t = \sin^{-1}\left(\sqrt{\frac{\epsilon_1}{\epsilon_2}}\sin\theta_i\right) \tag{8.63}$$

We shall now consider the derivation of the expressions for the reflection and transmission coefficients at the boundary. To do this, we distinguish between two cases: (1) the electric field vector of the wave linearly polarized parallel to the interface and (2) the magnetic field vector of the wave linearly polarized parallel to the interface. The law of reflection and Snell's law hold for both cases, since they result from the fact that the apparent phase velocities of the incident, reflected, and transmitted waves parallel to the boundary must be equal.

The geometry pertinent to the case of the electric field vector parallel to the interface is shown in Figure 8.17, in which the interface is assumed to be in the $x = 0$ plane and the subscripts i, r, and t associated with the field symbols denote incident, reflected, and transmitted waves, respectively. The plane of incidence, that is, the plane containing the normal to the interface and the propagation vectors, is assumed to be in the xz-plane, so that the electric field vectors are entirely in the y-direction. The corresponding magnetic field vectors are then as shown in the figure so as to be consistent

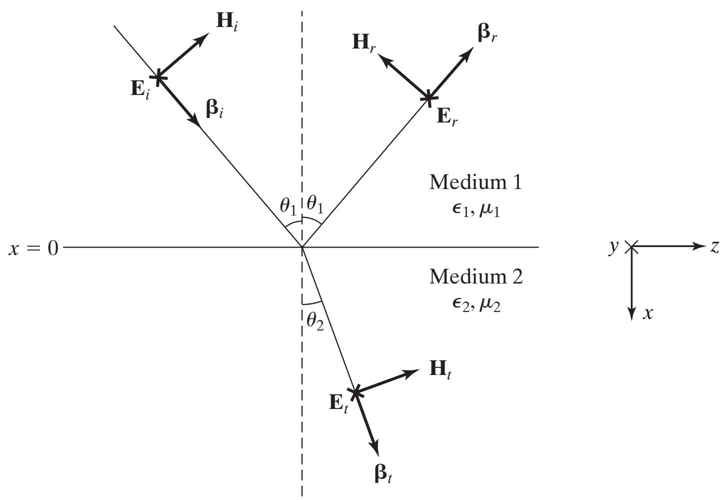

FIGURE 8.17

For obtaining the reflection and transmission coefficients for an obliquely incident uniform plane wave on a dielectric interface with its electric field perpendicular to the plane of incidence.

with the condition that **E**, **H**, and $\boldsymbol{\beta}$ form a right-handed mutually orthogonal set of vectors. Since the electric field vectors are perpendicular to the plane of incidence, this case is also said to correspond to perpendicular polarization. The angle of incidence is assumed to be θ_1. From the law of reflection (8.60), the angle of reflection is then also θ_1. The angle of transmission, assumed to be θ_2, is related to θ_1 by Snell's law, given by (8.61).

The boundary conditions to be satisfied at the interface $x = 0$ are that (1) the tangential component of the electric field intensity be continuous and (2) the tangential component of the magnetic field intensity be continuous. Thus, we have at the interface $x = 0$

$$E_{yi} + E_{yr} = E_{yt} \tag{8.64a}$$

$$H_{zi} + H_{zr} = H_{zt} \tag{8.64b}$$

Expressing the quantities in (8.64a) and (8.64b) in terms of the total fields, we obtain

$$E_i + E_r = E_t \tag{8.65a}$$

$$H_i \cos\theta_1 - H_r \cos\theta_1 = H_t \cos\theta_2 \tag{8.65b}$$

We also know from one of the properties of uniform plane waves that

$$\frac{E_i}{H_i} = \frac{E_r}{H_r} = \eta_1 = \sqrt{\frac{\mu_1}{\epsilon_1}} \tag{8.66a}$$

$$\frac{E_t}{H_t} = \eta_2 = \sqrt{\frac{\mu_2}{\epsilon_2}} \tag{8.66b}$$

Substituting (8.66a) and (8.66b) into (8.65b) and rearranging, we get

$$E_i - E_r = E_t \frac{\eta_1}{\eta_2} \frac{\cos\theta_2}{\cos\theta_1} \tag{8.67}$$

Solving (8.65a) and (8.67) for E_i and E_r, we have

$$E_i = \frac{E_t}{2}\left(1 + \frac{\eta_1}{\eta_2} \frac{\cos\theta_2}{\cos\theta_1}\right) \tag{8.68a}$$

$$E_r = \frac{E_t}{2}\left(1 - \frac{\eta_1}{\eta_2} \frac{\cos\theta_2}{\cos\theta_1}\right) \tag{8.68b}$$

We now define the reflection coefficient $\Gamma_\perp$ and the transmission coefficient $\tau_\perp$ as

$$\Gamma_\perp = \frac{E_r}{E_i} = \frac{E_{yr}}{E_{yi}} \tag{8.69a}$$

$$\tau_\perp = \frac{E_t}{E_i} = \frac{E_{yt}}{E_{yi}} \tag{8.69b}$$

where the subscript $\perp$ refers to perpendicular polarization. From (8.68a) and (8.68b), we then obtain

$$\Gamma_\perp = \frac{\eta_2 \cos\theta_1 - \eta_1 \cos\theta_2}{\eta_2 \cos\theta_1 + \eta_1 \cos\theta_2} \tag{8.70a}$$

$$\tau_\perp = \frac{2\eta_2 \cos\theta_1}{\eta_2 \cos\theta_1 + \eta_1 \cos\theta_2} \tag{8.70b}$$

Equations (8.70a) and (8.70b) are known as the *Fresnel reflection and transmission coefficients* for perpendicular polarization.

Before we discuss the result given by (8.70a) and (8.70b), we shall derive the corresponding expressions for the case in which the magnetic field of the wave is parallel to the interface. The geometry pertinent to this case is shown in Figure 8.18. Here again the plane of incidence is chosen to be the xz-plane, so that the magnetic field vectors are entirely in the y-direction. The corresponding electric field vectors are then as shown in the figure so as to be consistent with the condition that **E**, **H**, and $\boldsymbol{\beta}$ form a right-handed mutually orthogonal set of vectors. Since the electric field vectors are parallel to the plane of incidence, this case is also said to correspond to parallel polarization.

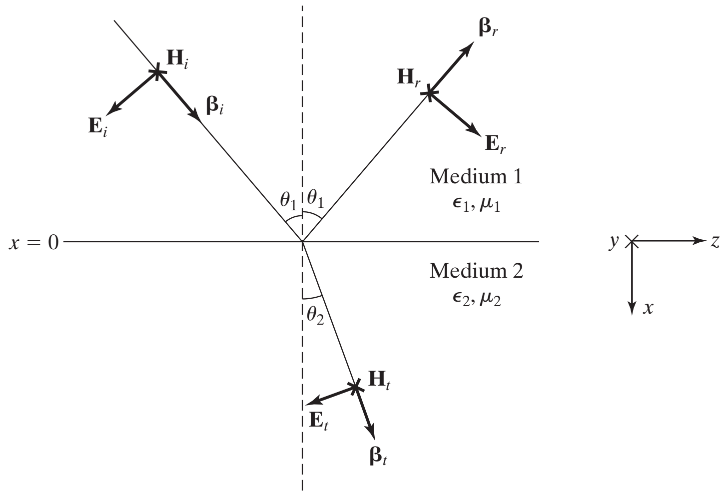

FIGURE 8.18

For obtaining the reflection and transmission coefficients for an obliquely incident uniform plane wave on a dielectric interface with its electric field parallel to the plane of incidence.

Once again the boundary conditions to be satisfied at the interface $x = 0$ are that (1) the tangential component of the electric field intensity be continuous and (2) the tangential component of the magnetic field intensity be continuous. Thus, we have at the interface $x = 0$,

$$E_{zi} + E_{zr} = E_{zt} \tag{8.71a}$$

$$H_{yi} + H_{yr} = H_{yt} \tag{8.71b}$$

Expressing the quantities in (8.71a) and (8.71b) in terms of the total fields and also using (8.66a) and (8.66b), we obtain

$$E_i - E_r = E_t \frac{\cos \theta_2}{\cos \theta_1} \tag{8.72a}$$

$$E_i + E_r = E_t \frac{\eta_1}{\eta_2} \tag{8.72b}$$

Solving (8.72a) and (8.72b) for E_i and E_r, we have

$$E_i = \frac{E_t}{2}\left(\frac{\eta_1}{\eta_2} + \frac{\cos \theta_2}{\cos \theta_1}\right) \tag{8.73a}$$

$$E_r = \frac{E_t}{2}\left(\frac{\eta_1}{\eta_2} - \frac{\cos \theta_2}{\cos \theta_1}\right) \tag{8.73b}$$

We now define the reflection coefficient $\Gamma_{\|}$ and the transmission coefficient $\tau_{\|}$ as

$$\Gamma_{\|} = -\frac{E_r}{E_i} \tag{8.74a}$$

$$\tau_{\|} = \frac{E_t}{E_i} \tag{8.74b}$$

where the subscript $\|$ refers to parallel polarization. From (8.73a) and (8.73b), we then obtain

$$\Gamma_{\|} = \frac{\eta_2 \cos \theta_2 - \eta_1 \cos \theta_1}{\eta_2 \cos \theta_2 + \eta_1 \cos \theta_1} \tag{8.75a}$$

$$\tau_{\|} = \frac{2\eta_2 \cos \theta_1}{\eta_2 \cos \theta_2 + \eta_1 \cos \theta_1} \tag{8.75b}$$

Note from (8.74a) and (8.74b) that

$$\frac{E_{zr}}{E_{zi}} = \frac{E_r \cos \theta_1}{-E_i \cos \theta_1} = -\frac{E_r}{E_i} = \Gamma_{\|} \tag{8.76a}$$

$$\frac{E_{zt}}{E_{zi}} = \frac{-E_t \cos \theta_2}{-E_i \cos \theta_1} = \tau_{\|} \frac{\cos \theta_2}{\cos \theta_1} \tag{8.76b}$$

Equations (8.75a) and (8.75b) are known as the *Fresnel reflection and transmission coefficients* for parallel polarization.

We shall now discuss the results given by (8.70a), (8.70b), (8.75a), and (8.75b) for the reflection and transmission coefficients for the two cases:

1. For $\theta_1 = 0$, that is, for the case of normal incidence of the uniform plane wave upon the interface, $\theta_2 = 0$ and

$$\Gamma_{\perp} = \frac{\eta_2 - \eta_1}{\eta_2 + \eta_1}, \qquad \Gamma_{\|} = \frac{\eta_2 - \eta_1}{\eta_2 + \eta_1}$$

$$\tau_{\perp} = \frac{2\eta_2}{\eta_2 + \eta_1}, \qquad \tau_{\|} = \frac{2\eta_2}{\eta_2 + \eta_1}$$

Thus, the reflection coefficients as well as the transmission coefficients for the two cases become equal as they should, since for normal incidence there is no difference between the two polarizations except for rotation by 90° parallel to the interface.

2. $\Gamma_\perp = 1$ and $\Gamma_\| = -1$ if $\cos\theta_2 = 0$; that is,

$$\sqrt{1 - \sin^2\theta_2} = \sqrt{1 - \frac{\mu_1\epsilon_1}{\mu_2\epsilon_2}\sin^2\theta_1} = 0$$

or

$$\sin\theta_1 = \sqrt{\frac{\mu_2\epsilon_2}{\mu_1\epsilon_1}} \tag{8.77}$$

where we have used Snell's law, given by (8.61), to express $\sin\theta_2$ in terms of $\sin\theta_1$. If we assume $\mu_2 = \mu_1 = \mu_0$, as is usually the case, (8.77) has real solutions for θ_1 for $\epsilon_2 < \epsilon_1$. Thus, for $\epsilon_2 < \epsilon_1$, that is, for transmission from a dielectric medium of higher permittivity into a dielectric medium of lower permittivity, there is a critical angle of incidence θ_c given by

$$\theta_c = \sin^{-1}\sqrt{\frac{\epsilon_2}{\epsilon_1}} \tag{8.78}$$

for which θ_2 is equal to 90° and $|\Gamma_\perp|$ and $|\Gamma_\|| = 1$. For $\theta_1 > \theta_c$, $\sin\theta_2$ becomes greater than 1, $\cos\theta_2$ becomes imaginary, and $\Gamma_\perp$ and $\Gamma_\|$ become complex, but with their magnitudes equal to unity, and *total internal reflection* occurs; that is, the time-average power of incident wave is entirely reflected, the boundary condition being satisfied by an evanescent field in medium 2. To explain the evanescent nature, we note with reference to the geometry of Figure 8.17 or Figure 8.18 that

$$\beta_{x2}^2 + \beta_{z2}^2 = \beta_t^2 = \omega^2\mu_2\epsilon_2$$

or

$$\beta_{x2}^2 = \omega^2\mu_2\epsilon_2 - \beta_{z2}^2$$

For $\theta_1 = \theta_c$, $\beta_{z2} = \beta_{z1} = \omega^2\mu_1\epsilon_1\sin^2\theta_c = \omega^2\mu_2\epsilon_2$, and $\beta_{x2}^2 = 0$. Therefore, for $\theta_1 > \theta_c$, $\beta_{z2} = \beta_{z1} = \omega^2\mu_1\epsilon_1\sin^2\theta_1 > \omega^2\mu_2\epsilon_2$, and $\beta_{x2}^2 < 0$. Thus, β_{x2} should be replaced by $-j\alpha_{x2}$, corresponding to exponential decay of the field in the x-direction without a propagating wave character. The phenomenon of total internal reflection is the fundamental principle of optical waveguides, since if we have a dielectric slab of permittivity ϵ_1 sandwiched between two dielectric media of permittivity $\epsilon_2 < \epsilon_1$, then by launching waves at an angle of incidence greater than the critical angle, it is possible to achieve guided wave propagation within the slab, as we shall learn in the next section.

3. $\Gamma_\perp = 0$ for $\eta_2\cos\theta_1 = \eta_1\cos\theta_2$; that is, for

$$\eta_2\sqrt{1 - \sin^2\theta_1} = \eta_1\sqrt{1 - \frac{\mu_1\epsilon_1}{\mu_2\epsilon_2}\sin^2\theta_1}$$

or

$$\sin^2 \theta_1 = \frac{\eta_2^2 - \eta_1^2}{\eta_2^2 - \eta_1^2(\mu_1\epsilon_1/\mu_2\epsilon_2)} = \mu_2 \frac{\mu_2 - \mu_1(\epsilon_2/\epsilon_1)}{\mu_2^2 - \mu_1^2} \tag{8.79}$$

For the usual case of transmission between two dielectric materials, that is, for $\mu_2 = \mu_1$ and $\epsilon_2 \neq \epsilon_1$, this equation has no real solution for θ_1, and hence there is no angle of incidence for which the reflection coefficient is zero for the case of perpendicular polarization.

4. $\Gamma_{\|} = 0$ for $\eta_2 \cos\theta_2 = \eta_1 \cos\theta_1$; that is, for

$$\eta_2 \sqrt{1 - \frac{\mu_1\epsilon_1}{\mu_2\epsilon_2}\sin^2\theta_1} = \eta_1\sqrt{1 - \sin^2\theta_1}$$

or

$$\sin^2 \theta_1 = \frac{\eta_2^2 - \eta_1^2}{\eta_2^2(\mu_1\epsilon_1/\mu_2\epsilon_2) - \eta_1^2} = \epsilon_2 \frac{(\mu_2/\mu_1)\epsilon_1 - \epsilon_2}{\epsilon_1^2 - \epsilon_2^2} \tag{8.80}$$

If we assume $\mu_2 = \mu_1$, this equation reduces to

$$\sin^2\theta_1 = \frac{\epsilon_2}{\epsilon_1 + \epsilon_2}$$

which then gives

$$\cos^2\theta_1 = 1 - \sin^2\theta_1 = \frac{\epsilon_1}{\epsilon_1 + \epsilon_2}$$

and

$$\tan\theta_1 = \sqrt{\frac{\epsilon_2}{\epsilon_1}}$$

Thus, there exists a value of the angle of incidence θ_p, given by

$$\theta_p = \tan^{-1}\sqrt{\frac{\epsilon_2}{\epsilon_1}} \tag{8.81}$$

for which the reflection coefficient is zero, and hence there is complete transmission for the case of parallel polarization.

5. In view of cases 3 and 4, for an elliptically polarized wave incident on the interface at the angle θ_p, the reflected wave will be linearly polarized perpendicular to the plane of incidence. For this reason, the angle θ_p is known as the *polarizing angle*. It is also known as the *Brewster angle*. The phenomenon associated with the Brewster angle has several applications. An example is in gas lasers in which the discharge tube lying between the mirrors of a Fabry–Perot resonator is sealed

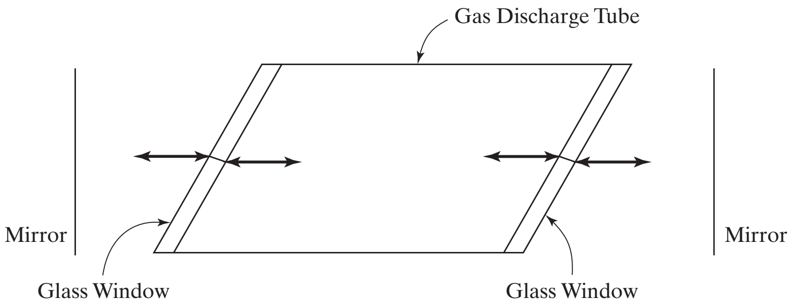

FIGURE 8.19

For illustrating the application of the Brewster angle effect in gas lasers.

by glass windows placed at the Brewster angle, as shown in Figure 8.19, to minimize reflections from the ends of the tube so that the laser behavior is governed by the mirrors external to the tube.

We shall now consider an example.

Example 8.5

A uniform plane wave having the electric field

$$\mathbf{E}_i = E_0\left(\frac{\sqrt{3}}{2}\mathbf{a}_x - \frac{1}{2}\mathbf{a}_z\right)\cos\,[6\pi \times 10^9 t - 10\pi(x + \sqrt{3}z)]$$

is incident on the interface between free space and a dielectric medium of $\epsilon = 1.5\epsilon_0$ and $\mu = \mu_0$, as shown in Figure 8.20. We wish to obtain the expressions for the electric fields of the reflected and transmitted waves.

First, we note from the given $\mathbf{E}_i$ that the propagation vector of the incident wave is given by

$$\boldsymbol{\beta}_i = 10\pi(\mathbf{a}_x + \sqrt{3}\mathbf{a}_z) = 20\pi\left(\frac{1}{2}\mathbf{a}_x + \frac{\sqrt{3}}{2}\mathbf{a}_z\right)$$

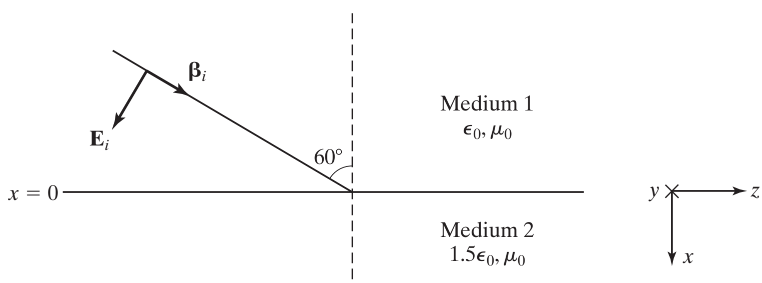

FIGURE 8.20

For Example 8.5.

the direction of which is consistent with the angle of incidence of 60°. We also note that the electric field vector (which is perpendicular to $\boldsymbol{\beta}_i$) is entirely in the plane of incidence. Thus, the situation corresponds to one of parallel polarization, as in Figure 8.18.

To obtain the required fields, we first find, by using (8.63) and with reference to the notation of Figure 8.18, that

$$\sin\theta_2 = \sqrt{\frac{\epsilon_0}{1.5\epsilon_0}}\sin 60^\circ = \frac{1}{\sqrt{2}}$$

or $\theta_2 = 45°$. Then from (8.75a)–(8.75b) and (8.76a)–(8.76b), we have

$$\begin{aligned}
\Gamma_\parallel &= \frac{(\eta_0/\sqrt{1.5})\cos 45^\circ - \eta_0\cos 60^\circ}{(\eta_0/\sqrt{1.5})\cos 45^\circ + \eta_0\cos 60^\circ} \\
&= \frac{2-\sqrt{3}}{2+\sqrt{3}} = 0.072 \\
\tau_\parallel &= \frac{2(\eta_0/\sqrt{1.5})\cos 60^\circ}{(\eta_0/\sqrt{1.5})\cos 45^\circ + \eta_0\cos 60^\circ} \\
&= \frac{2\sqrt{2}}{2+\sqrt{3}} = 0.758 \\
\frac{E_r}{E_i} &= -0.072 \\
\frac{E_t}{E_i} &= 0.758
\end{aligned}$$

Finally, noting with the aid of Figure 8.21 that

$$\boldsymbol{\beta}_r = 20\pi\left(-\frac{1}{2}\mathbf{a}_x + \frac{\sqrt{3}}{2}\mathbf{a}_z\right) = 10\pi(-\mathbf{a}_x + \sqrt{3}\mathbf{a}_z)$$

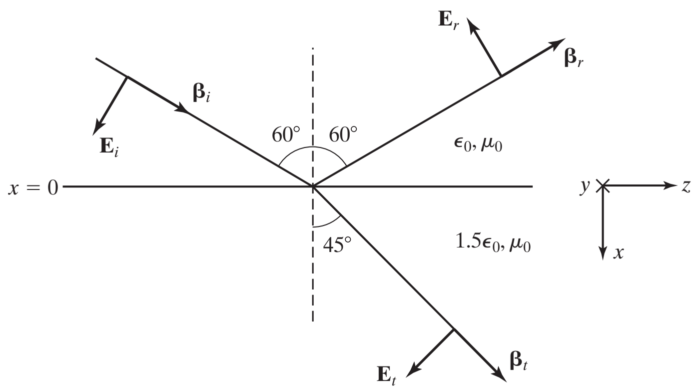

FIGURE 8.21

For writing the expressions for the reflected and transmitted wave electric fields for Example 8.5.

and

$$\boldsymbol{\beta}_t = 20\pi\sqrt{1.5}\left(\frac{1}{\sqrt{2}}\mathbf{a}_x + \frac{1}{\sqrt{2}}\mathbf{a}_z\right) = 10\sqrt{3}\pi(\mathbf{a}_x + \mathbf{a}_z)$$

we write the expressions for the reflected and transmitted wave fields to be

$$\mathbf{E}_r = -0.072E_0\left(\frac{\sqrt{3}}{2}\mathbf{a}_x + \frac{1}{2}\mathbf{a}_z\right)\cos\,[6\pi \times 10^9 t + 10\pi(x - \sqrt{3}z)]$$

and

$$\mathbf{E}_t = 0.758E_0\left(\frac{1}{\sqrt{2}}\mathbf{a}_x - \frac{1}{\sqrt{2}}\mathbf{a}_z\right)\cos\,[6\pi \times 10^9 t - 10\sqrt{3}\pi(x + z)]$$

Note that for $x = 0$, $E_{zi} + E_{zr} = E_{zt}$ and $E_{xi} + E_{xr} = 1.5E_{xt}$, so that the fields do indeed satisfy the boundary conditions.

8.6 DIELECTRIC SLAB GUIDE

In the preceding section, we learned that for a wave that is incident obliquely from a dielectric medium of permittivity ϵ_1 onto another dielectric medium of permittivity $\epsilon_2 < \epsilon_1$, total internal reflection occurs for angles of incidence θ_i exceeding the critical angle θ_c given by

$$\theta_c = \sin^{-1}\sqrt{\frac{\epsilon_2}{\epsilon_1}} \tag{8.82}$$

where it is assumed that $\mu = \mu_0$ everywhere. In this section, we shall consider the dielectric slab waveguide, which forms the basis for thin-film waveguides, used extensively in integrated optics.

The dielectric slab waveguide consists of a dielectric slab of permittivity ϵ_1, sandwiched between two dielectric media of permittivities less than ϵ_1. For simplicity, we shall consider the symmetric waveguide, that is, one for which the permittivities of the dielectrics on either side of the slab are the same and equal to ϵ_2, as shown in Figure 8.22. Then by launching waves at an angle of incidence $\theta_i > \theta_c$, where θ_c is given by (8.82), it is possible to achieve guided wave propagation within the slab, as shown in the figure. For a given thickness d of the slab and for a given frequency of the waves, there are only discrete values of θ_i for which the guiding can take place. In other words, guiding of a wave of a given frequency is not ensured simply because the condition for total internal reflection is met.

The allowed values of θ_i are dictated by the self-consistency condition, which can be explained with the aid of the construction in Figure 8.23, as follows. If we consider a point A on a given wavefront designated 1 and follow that wavefront as it moves to position $1'$ passing through point B, reflects at the interface $x = d/2$ giving rise to

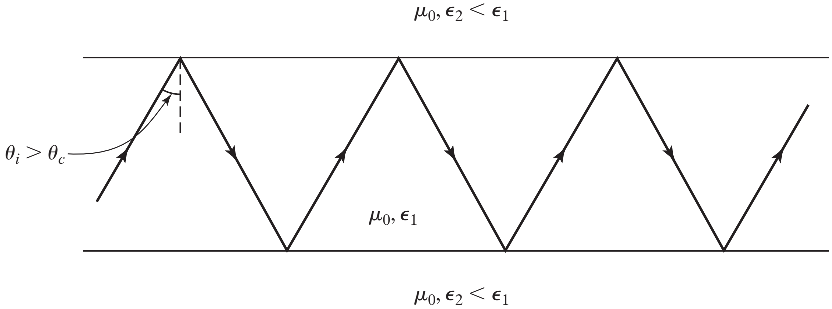

FIGURE 8.22

Total internal reflection in a dielectric slab waveguide.

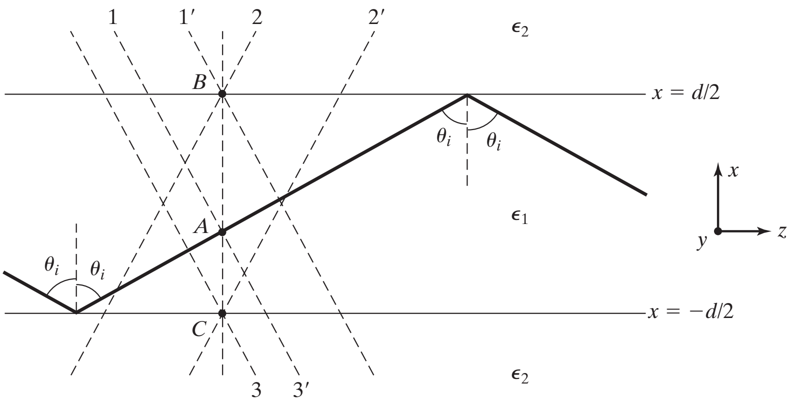

FIGURE 8.23

For explaining the self-consistency condition for waveguiding in a dielectric slab guide.

wavefront designated 2, then moves to position 2′ passing through point C, reflects at the interface $x = -d/2$ giving rise to wavefront designated 3, and finally moves to position 3′ passing through A, then we see that the total phase shift undergone must be equal to an integer multiple of 2π. If λ_0 is the wavelength in free space corresponding to the wave frequency, the self-consistency condition is given by

$$\frac{2\pi\sqrt{\epsilon_{r1}}}{\lambda_0}(AB\cos\theta_i) + \underline{/\bar{\Gamma}_B} + \frac{2\pi\sqrt{\epsilon_{r1}}}{\lambda_0}(BC\cos\theta_i)$$
$$+ \underline{/\bar{\Gamma}_A} + \frac{2\pi\sqrt{\epsilon_{r1}}}{\lambda_0}(CA\cos\theta_i) = 2m\pi, \qquad m = 0, 1, 2, \ldots \tag{8.83}$$

where $\bar{\Gamma}_A$ and $\bar{\Gamma}_B$ are the reflection coefficients at the interfaces $x = -d/2$ and $x = d/2$, respectively, and $\epsilon_{r1} = \epsilon_1/\epsilon_0$. We recall that under conditions of total internal reflection, the reflection coefficients (8.70a) and (8.75a) become complex with their magnitudes equal to unity. For the symmetric waveguide, $\bar{\Gamma}_A = \bar{\Gamma}_B$. Thus, substituting $\bar{\Gamma}$ for $\bar{\Gamma}_A$ and $\bar{\Gamma}_B$ and $2d$ for $(AB + BC + CA)$, we write (8.83) as

$$\frac{4\pi d\sqrt{\epsilon_{r1}}}{\lambda_0}\cos\theta_i + 2\underline{/\bar{\Gamma}} = 2m\pi, \qquad m = 0, 1, 2, \ldots$$

or

$$\frac{2\pi d\sqrt{\epsilon_{r1}}}{\lambda_0}\cos\theta_i + \underline{/\bar{\Gamma}} = m\pi, \qquad m = 0, 1, 2, \ldots \tag{8.84}$$

To proceed further, we need to distinguish between the cases of perpendicular and parallel polarizations as defined in the preceding section, since the reflection coefficients for the two cases are different. We shall here consider only the case of perpendicular polarization. The situation then corresponds to TE modes, since the electric field has no longitudinal or z-component. Thus, substituting

$$\cos\theta_1 = \cos\theta_i$$

and

$$\begin{aligned}\cos\theta_2 &= \sqrt{1 - \sin^2\theta_2}\\ &= j\sqrt{\sin^2\theta_2 - 1}\\ &= j\sqrt{\frac{\epsilon_1}{\epsilon_2}\sin^2\theta_i - 1}\end{aligned}$$

in (8.70a), we obtain

$$\bar{\Gamma}_\perp = \frac{\eta_2\cos\theta_i - j\eta_1\sqrt{(\epsilon_1/\epsilon_2)\sin^2\theta_i - 1}}{\eta_2\cos\theta_i + j\eta_1\sqrt{(\epsilon_1/\epsilon_2)\sin^2\theta_i - 1}} \tag{8.85}$$

so that

$$\begin{aligned}\underline{/\bar{\Gamma}_\perp} &= -2\tan^{-1}\frac{\eta_1\sqrt{(\epsilon_1/\epsilon_2)\sin^2\theta_i - 1}}{\eta_2\cos\theta_i}\\ &= -2\tan^{-1}\frac{\sqrt{\sin^2\theta_i - (\epsilon_2/\epsilon_1)}}{\cos\theta_i}\end{aligned} \tag{8.86}$$

Substituting (8.86) into (8.84), we then obtain

$$\frac{2\pi d\sqrt{\epsilon_{r1}}}{\lambda_0}\cos\theta_i - 2\tan^{-1}\frac{\sqrt{\sin^2\theta_i - (\epsilon_2/\epsilon_1)}}{\cos\theta_i} = m\pi, \qquad m = 0, 1, 2, \ldots$$

or

$$\tan\left(\frac{\pi d\sqrt{\epsilon_{r1}}}{\lambda_0}\cos\theta_i - \frac{m\pi}{2}\right) = \frac{\sqrt{\sin^2\theta_i - (\epsilon_2/\epsilon_1)}}{\cos\theta_i}, \qquad m = 0, 1, 2, \ldots$$

or

$$\tan[f(\theta_i)] = \begin{cases} g(\theta_i), & m = 0, 2, 4, \ldots \\ -\dfrac{1}{g(\theta_i)}, & m = 1, 3, 5, \ldots \end{cases} \tag{8.87}$$

where

$$f(\theta_i) = \frac{\pi d\sqrt{\epsilon_{r1}}}{\lambda_0}\cos\theta_i \tag{8.88a}$$

$$g(\theta_i) = \frac{\sqrt{\sin^2\theta_i - (\epsilon_2/\epsilon_1)}}{\cos\theta_i} \tag{8.88b}$$

Equation (8.87) is the characteristic equation for the guiding of TE waves in the dielectric slab. For given values of ϵ_1, ϵ_2, d, and λ_0, the solutions for θ_i can be obtained by plotting the two sides of (8.87) versus θ_i and finding the points of intersection. The nature of this construction is shown in Figure 8.24. Each solution corresponds to one

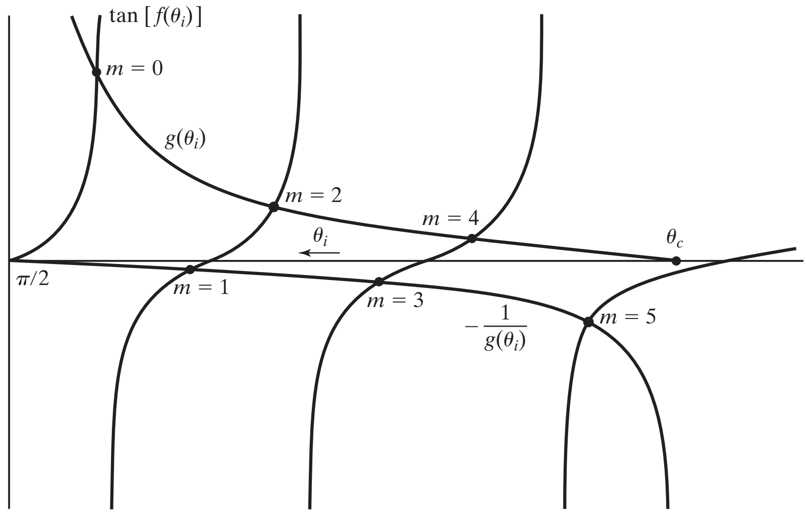

FIGURE 8.24

Graphical construction pertinent to the solution of equation (8.87).

mode. It can be seen from (8.88a) and Figure 8.24 that for a given set of values of ϵ_1 and ϵ_2, fewer solutions are obtained for θ_i as the ratio (d/λ_0) becomes smaller, since the number of branches of the plot of tan $[f(\theta_i)]$ between $\theta_i = \pi/2$ and $\theta_i = \theta_c$ become fewer. It can also be seen that there is always one solution for a given d, even for arbitrarily low values of (d/λ_0)—that is, for large values of λ_0 or low frequencies.

Alternative to the graphical solution, we can use a computer to solve (8.87) for the allowed values of θ_i for specified values of ϵ_{r1}, ϵ_{r2}, d, and λ_0. Computed values of θ_i for values of $\epsilon_{r1} = 4$, $\epsilon_{r2} = 1$, $d = 10$ mm, and $\lambda_0 = 5$ mm are listed in Table 8.1.

TABLE 8.1 Allowed Values of θ_i for Dielectric Slab Guide Example

m	θ_i (deg)
0	83.42783
1	76.77756
2	69.96263
3	62.87805
4	55.38428
5	47.28283
6	38.30225

Returning now to Figure 8.24, we designate the modes associated with the solutions as TE_m modes, where $m = 0, 1, 2, \ldots$ correspond to the values of m on the plot. We note from the plot that the solution for a given TE_m mode for $m > 1$ does not exist if $f(\theta_c) < m\pi/2$. Therefore, the cutoff condition is given by

$$\frac{\pi d\sqrt{\epsilon_{r1}}}{\lambda_0}\cos\theta_c < \frac{m\pi}{2}$$

$$\frac{\pi d\sqrt{\epsilon_{r1}}}{\lambda_0}\sqrt{1 - \frac{\epsilon_2}{\epsilon_1}} < \frac{m\pi}{2}$$

$$\lambda_0 > \frac{2d\sqrt{\epsilon_{r1} - \epsilon_{r2}}}{m} \tag{8.89}$$

where we have used (8.82). The cutoff frequency is given by

$$f_c = \frac{c}{\lambda_0} = \frac{mc}{2d\sqrt{\epsilon_{r1} - \epsilon_{r2}}}$$

The fundamental mode, TE_0, has no cutoff frequency. Thus,

$$f_c = \frac{mc}{2d\sqrt{\epsilon_{r1} - \epsilon_{r2}}}, \qquad m = 0, 1, 2, \ldots \tag{8.90}$$

Example 8.6

For the symmetric dielectric slab waveguide of Figure 8.23, let $\epsilon_1 = 2.56\epsilon_0$, $\epsilon_2 = \epsilon_0$, and $d = 10\lambda_0$. We wish to find the number of TE modes that can propagate by guidance in the slab.

From (8.90),

$$f_c = \frac{mc}{20\lambda_0\sqrt{2.56 - 1}}$$

$$= \frac{mf}{24.98}, \qquad m = 0, 1, 2, \ldots$$

Thus, for $m > 24$, $f_c > f$ and the modes are cut off. Therefore, the number of propagating TE modes is 25, corresponding to $m = 0, 1, 2, \ldots, 24$.

The entire discussion for guided waves in the dielectric slab guide can be repeated for TM modes by using $\overline{\Gamma}_{\|}$ in the place of $\overline{\Gamma}_{\perp}$ in (8.84) to derive the characteristic equation for guidance. We shall include the derivation as Problem 8.32, and conclude this section with a brief description of an optical fiber, which is a common form of optical waveguide.

An optical fiber, so termed because of its filamentary appearance, consists typically of a core and a cladding, having cylindrical cross sections as shown in Figure 8.25(a). The core is made up of a material of permittivity greater than that of the cladding so that a critical angle exists for waves inside the core incident on the interface between the core and the cladding, and hence waveguiding is made possible in the core by total internal reflection. The phenomenon may be visualized by considering a longitudinal cross section of the fiber through its axis, shown in Figure 8.25(b), and comparing it with that of the slab waveguide, shown in Figure 8.22. Although the cladding is not essential for the purpose of waveguiding in the core, since the permittivity of the core material is greater than that of free space, it serves two useful purposes: (a) It avoids scattering and field distortion by the supporting structure of the fiber, since the field decays exponentially outside the core, and hence is negligible outside the cladding. (b) It allows single-mode propagation for a larger value of the radius of the core than permitted in the absence of the cladding.

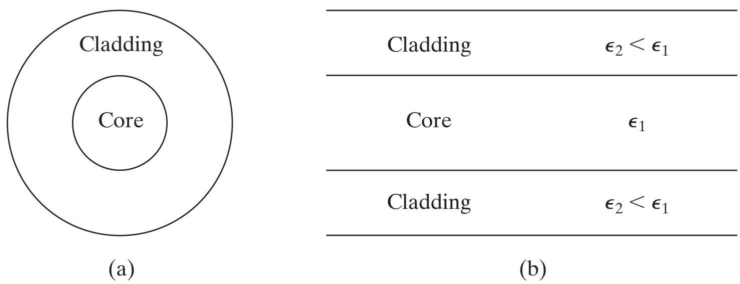

FIGURE 8.25

(a) Transverse and (b) longitudinal cross sections of an optical fiber.

SUMMARY

In this chapter, we studied the principles of waveguides. To introduce the waveguiding phenomenon, we first learned how to write the expressions for the electric and magnetic fields of a uniform plane wave propagating in an arbitrary direction with respect to the coordinate axes. These expressions are given by

$$\mathbf{E} = \mathbf{E}_0 \cos(\omega t - \boldsymbol{\beta} \cdot \mathbf{r} + \phi_0)$$
$$\mathbf{H} = \mathbf{H}_0 \cos(\omega t - \boldsymbol{\beta} \cdot \mathbf{r} + \phi_0)$$

where $\boldsymbol{\beta}$ and $\mathbf{r}$ are the propagation and position vectors given by

$$\boldsymbol{\beta} = \beta_x \mathbf{a}_x + \beta_y \mathbf{a}_y + \beta_z \mathbf{a}_z$$
$$\mathbf{r} = x\mathbf{a}_x + y\mathbf{a}_y + z\mathbf{a}_z$$

and ϕ_0 is the phase of the wave at the origin at $t = 0$. The magnitude of $\boldsymbol{\beta}$ is equal to $\omega\sqrt{\mu\epsilon}$, the phase constant along the direction of propagation of the wave. The direction of $\boldsymbol{\beta}$ is the direction of propagation of the wave. We learned that

$$\mathbf{E}_0 \cdot \boldsymbol{\beta} = 0$$
$$\mathbf{H}_0 \cdot \boldsymbol{\beta} = 0$$
$$\mathbf{E}_0 \cdot \mathbf{H}_0 = 0$$

that is, $\mathbf{E}_0$, $\mathbf{H}_0$, and $\boldsymbol{\beta}$ are mutually perpendicular, and that

$$\frac{|\mathbf{E}_0|}{|\mathbf{H}_0|} = \eta = \sqrt{\frac{\mu}{\epsilon}}$$

Also, since $\mathbf{E} \times \mathbf{H}$ should be directed along the propagation vector $\boldsymbol{\beta}$, it then follows that

$$\mathbf{H} = \frac{1}{\omega\mu}\boldsymbol{\beta} \times \mathbf{E}$$

The quantities β_x, β_y, and β_z are the phase constants along the x-, y-, and z-axes, respectively. The apparent wavelengths and the apparent phase velocities along the coordinate axes are given, respectively, by

$$\lambda_i = \frac{2\pi}{\beta_i}, \qquad i = x, y, z$$
$$v_{pi} = \frac{\omega}{\beta_i}, \qquad i = x, y, z$$

By considering the superposition of two uniform plane waves propagating at an angle to each other and placing two perfect conductors in appropriate planes such that the boundary condition of zero tangential electric field is satisfied, we introduced the parallel-plate waveguide. We learned that the composite wave is a transverse electric wave, or TE wave, since the electric field is entirely transverse to the direction of time-average power flow, that is, the guide axis, but the magnetic field is not. In terms of the uniform plane wave propagation, the phenomenon is one of waves bouncing obliquely between the conductors as they progress down the guide. For a fixed spacing a between the conductors of the guide, waves of different frequencies bounce obliquely at different angles such that the spacing a is equal to an integer, say, m number of one-half apparent wavelengths normal to the plates and hence the fields have m number of one-half-sinusoidal variations normal to the plates. These are said to correspond to $\text{TE}_{m,0}$ modes, where the subscript 0 implies no variations of the fields in the direction parallel to the plates and transverse to the guide axis. When the frequency is such that the spacing a is equal to m one-half wavelengths, the waves bounce normally to the plates without the feeling of being guided along the axis, thereby leading to the cutoff condition. Thus, the cutoff wavelengths corresponding to $\text{TE}_{m,0}$ modes are given by

$$\lambda_c = \frac{2a}{m}$$

and the cutoff frequencies are given by

$$f_c = \frac{v_p}{\lambda_c} = \frac{m}{2a\sqrt{\mu\epsilon}}$$

A given frequency signal can propagate in all modes for which $\lambda < \lambda_c$ or $f > f_c$. For the propagating range of frequencies, the wavelength along the guide axis, that is, the guide wavelength, and the phase velocity along the guide axis are given, respectively, by

$$\lambda_g = \frac{\lambda}{\sqrt{1 - (\lambda/\lambda_c)^2}} = \frac{\lambda}{\sqrt{1 - (f_c/f)^2}}$$

$$v_{pz} = \frac{v_p}{\sqrt{1 - (\lambda/\lambda_c)^2}} = \frac{v_p}{\sqrt{1 - (f_c/f)^2}}$$

We discussed the phenomenon of dispersion arising from the frequency dependence of the phase velocity along the guide axis, and we introduced the concept of group velocity. Group velocity is the velocity with which the envelope of a narrowband modulated signal travels in the dispersive channel, and hence it is the velocity with which the information is transmitted. It is given by

$$v_g = \frac{d\omega}{d\beta_z} = v_p\sqrt{1 - \left(\frac{f_c}{f}\right)^2}$$

where β_z is the phase constant along the guide axis.

We extended the treatment of the parallel-plate waveguide to the rectangular waveguide, which is a metallic pipe of rectangular cross section. By considering a rectangular waveguide of cross-sectional dimensions a and b, we discussed transverse electric or TE modes as well as transverse magnetic or TM modes, and learned that while $\text{TE}_{m,n}$ modes can include values of m or n equal to zero, $\text{TM}_{m,n}$ modes require that both m and n be nonzero, where m and n refer to the number of one-half sinusoidal variations of the fields along the dimensions a and b, respectively. The cutoff wavelengths for the $\mathrm{TE}_{m,n}$ or $\mathrm{TM}_{m,n}$ modes are given by

$$\lambda_c = \frac{1}{\sqrt{(m/2a)^2 + (n/2b)^2}}$$

The mode that has the largest cutoff wavelength or the lowest cutoff frequency is the dominant mode, which here is the $\mathrm{TE}_{1,0}$ mode. Waveguides are generally designed to transmit only the dominant mode.

By placing perfect conductors in two transverse planes of a rectangular waveguide separated by an integer multiple of one-half the guide wavelength, we introduced the cavity resonator, which is the microwave counterpart of the lumped parameter resonant circuit encountered in low-frequency circuit theory. For a rectangular cavity resonator having dimensions a, b, and d, the frequencies of oscillation for the $\mathrm{TE}_{m,n,l}$ or $\mathrm{TM}_{m,n,l}$ modes are given by

$$f_{\text{osc}} = \frac{1}{\sqrt{\mu\epsilon}}\sqrt{\left(\frac{m}{2a}\right)^2 + \left(\frac{n}{2b}\right)^2 + \left(\frac{l}{2d}\right)^2}$$

where l refers to the number of one-half sinusoidal variations of the fields along the dimension d.

We then considered oblique incidence of a uniform plane wave on the boundary between two perfect dielectric media. We derived the *laws of reflection and refraction*, given, respectively, by

$$\theta_r = \theta_i$$

$$\theta_t = \sin^{-1}\left(\sqrt{\frac{\mu_1\epsilon_1}{\mu_2\epsilon_2}}\sin\theta_i\right)$$

where θ_i, θ_r, and θ_t are the angles of incidence, reflection, and transmission, respectively, of a uniform plane wave incident from medium 1 (ϵ_1, μ_1) onto medium 2 (ϵ_2, μ_2). The law of refraction is also known as *Snell's law*. We then derived the expressions for the reflection and transmission coefficients for the cases of perpendicular and parallel polarizations. An examination of these expressions revealed the following, under the assumption of $\mu_1 = \mu_2$: (1) for incidence from a medium of higher permittivity onto one of lower permittivity, there is a critical angle of incidence given by

$$\theta_c = \sin^{-1}\sqrt{\frac{\epsilon_2}{\epsilon_1}}$$

beyond which total internal reflection occurs, and (2) for the case of parallel polarization, there is an angle of incidence, known as the *Brewster angle* and given by

$$\theta_p = \tan^{-1}\sqrt{\frac{\epsilon_2}{\epsilon_1}}$$

for which the reflection coefficient is zero.

Next, we introduced the dielectric slab waveguide, consisting of a dielectric slab of permittivity ϵ_1 sandwiched between two dielectric media of permittivities $\epsilon_2 < \epsilon_1$.

We learned that by launching waves at an angle of incidence θ_i greater than the critical angle for total internal reflection, it is possible to achieve guided wave propagation within the slab. For a given frequency, several modes are possible corresponding to values of θ_i that satisfy the self-consistency condition associated with the bouncing waves. We derived the characteristic equation for computing these values of θ_i for the TE case and discussed its solution. The modes are designated TE_m modes and their cutoff frequencies are given by

$$f_c = \frac{mc}{2d\sqrt{\epsilon_{r1} - \epsilon_{r2}}}, \qquad m = 0, 1, 2, \ldots$$

where d is the thickness of the slab. The fundamental mode, TE_0, has no cutoff frequency. We concluded the discussion with a description of the optical fiber.

REVIEW QUESTIONS

8.1. What is the propagation vector? Interpret the significance of its magnitude and direction.

8.2. Discuss how the phase constants along the coordinate axes are less than the phase constant along the direction of propagation of a uniform plane wave propagating in an arbitrary direction.

8.3. Write the expressions for the electric and magnetic fields of a uniform plane wave propagating in an arbitrary direction and list all the conditions to be satisfied by the electric field, magnetic field, and propagation vectors.

8.4. What are apparent wavelengths? Why are they longer than the wavelength along the direction of propagation?

8.5. What are apparent phase velocities? Why are they greater than the phase velocity along the direction of propagation?

8.6. Discuss how the superposition of two uniform plane waves propagating at an angle to each other gives rise to a composite wave consisting of standing waves traveling bodily transverse to the standing waves.

8.7. What is a transverse electric wave? Discuss the reasoning behind the nomenclature $\mathrm{TE}_{m,0}$ modes.

8.8. How would you characterize a transverse magnetic wave?

8.9. Compare the phenomenon of guiding of uniform plane waves in a parallel-plate waveguide with that in a parallel-plate transmission line.

8.10. Discuss how the cutoff condition arises in a waveguide.

8.11. Explain the relationship between the cutoff wavelength and the spacing between the plates of a parallel-plate waveguide based on the phenomenon at cutoff.

8.12. Is the cutoff wavelength dependent on the dielectric in the waveguide? Is the cutoff frequency dependent on the dielectric in the waveguide?

8.13. What is guide wavelength?

8.14. Provide a physical explanation for the frequency dependence of the phase velocity along the guide axis.

8.15. Discuss the phenomenon of dispersion.

8.16. Discuss the concept of group velocity with the aid of an example.

8.17. What is a dispersion diagram? Explain how the phase and group velocities can be determined from a dispersion diagram.

8.18. When is it meaningful to attribute a group velocity to a signal comprised of more than two frequencies? Why?

8.19. Discuss the propagation of a narrow-band amplitude modulated signal in a dispersive channel.

8.20. Discuss the nomenclature associated with the modes of propagation in a rectangular waveguide.

8.21. Explain the relationship between the cutoff wavelength and the dimensions of a rectangular waveguide based on the phenomenon at cutoff.

8.22. Why can there be no transverse magnetic modes having no variations for the fields along one of the dimensions of a rectangular waveguide?

8.23. What is meant by the dominant mode? Why are waveguides designed so that they propagate only the dominant mode?

8.24. Why is the dimension b of a rectangular waveguide generally chosen to be less than or equal to one-half the dimension a?

8.25. What is a cavity resonator?

8.26. How do the dimensions of a rectangular cavity resonator determine the frequencies of oscillation of the resonator?

8.27. Discuss the condition required to be satisfied by the incident, reflected, and transmitted waves at the interface between two dielectric media.

8.28. What is Snell's law?

8.29. What is meant by the plane of incidence? Distinguish between the two different linear polarizations pertinent to the derivation of the reflection and transmission coefficients for oblique incidence on a dielectric interface.

8.30. Briefly discuss the determination of the Fresnel reflection and transmission coefficients for an obliquely incident wave on a dielectric interface.

8.31. What is total internal reflection? Discuss the nature of the reflection coefficient and the manner in which the boundary condition is satisfied for an angle of incidence greater than the critical angle for total internal reflection.

8.32. What is the Brewster angle? What is the polarization of the reflected wave for an elliptically polarized wave incident on a dielectric interface at the Brewster angle? Discuss an application of the Brewster angle effect.

8.33. Discuss the principle of optical waveguides by considering the dielectric slab waveguide.

8.34. Explain the self-consistency condition for waveguiding in a dielectric slab waveguide.

8.35. Discuss the dependence of the number of propagating modes in a dielectric slab waveguide on the ratio of the thickness d of the dielectric slab to the wavelength λ_0.

8.36. Considering TE modes in a dielectric slab guide, specify the fundamental mode and discuss the associated cutoff condition.

8.37. Compare the phenomenon at cutoff in a metallic waveguide with that at cutoff in an optical waveguide.

8.38. Provide a brief description of an optical fiber.

PROBLEMS

8.1. Assuming the x- and y-axes to be directed eastward and northward, respectively, find the expression for the propagation vector of a uniform plane wave of frequency 15 MHz in free space propagating in the direction 30° north of east.

8.2. The propagation vector of a uniform plane wave in a perfect dielectric medium having $\epsilon = 4.5\epsilon_0$ and $\mu = \mu_0$ is given by

$$\boldsymbol{\beta} = 2\pi(3\mathbf{a}_x + 4\mathbf{a}_y + 5\mathbf{a}_z)$$

Find (a) the apparent wavelengths and (b) the apparent phase velocities, along the coordinate axes.

8.3. For a uniform plane wave propagating in free space, the apparent phase velocities along the x- and y-directions are found to be $6\sqrt{2} \times 10^8$ m/s and $2\sqrt{3} \times 10^8$ m/s, respectively. Find the direction of propagation of the wave.

8.4. The electric field vector of a uniform plane wave propagating in a perfect dielectric medium having $\epsilon = 9\epsilon_0$ and $\mu = \mu_0$ is given by

$$\mathbf{E} = 10(-\mathbf{a}_x - 2\sqrt{3}\mathbf{a}_y + \sqrt{3}\mathbf{a}_z)\cos[16\pi \times 10^6 t - 0.04\pi(\sqrt{3}x - 2y - 3z)]$$

Find (a) the frequency, (b) the direction of propagation, (c) the wavelength along the direction of propagation, (d) the apparent wavelengths along the x-, y-, and z-axes, and (e) the apparent phase velocities along the x-, y-, and z-axes.

8.5. Given

$$\mathbf{E} = 10\mathbf{a}_x \cos[6\pi \times 10^7 t - 0.1\pi(y + \sqrt{3}z)]$$

(a) Determine if the given $\mathbf{E}$ represents the electric field of a uniform plane wave propagating in free space. (b) If the answer to part (a) is *yes*, find the corresponding magnetic field vector $\mathbf{H}$.

8.6. Given

$$\mathbf{E} = (\mathbf{a}_x - 2\mathbf{a}_y - \sqrt{3}\mathbf{a}_z)\cos[15\pi \times 10^6 t - 0.05\pi(\sqrt{3}x + z)]$$

$$\mathbf{H} = \frac{1}{60\pi}(\mathbf{a}_x + 2\mathbf{a}_y - \sqrt{3}\mathbf{a}_z)\cos[15\pi \times 10^6 t - 0.05\pi(\sqrt{3}x + z)]$$

(a) Perform all the necessary tests and determine if these fields represent a uniform plane wave propagating in a perfect dielectric medium. (b) Find the permittivity and the permeability of the medium.

8.7. Two equal-amplitude uniform plane waves of frequency 25 MHz and having their electric fields along the y-direction propagate along the directions $\mathbf{a}_z$ and $\frac{1}{2}(\sqrt{3}\mathbf{a}_x + \mathbf{a}_z)$ in free space. (a) Find the direction of propagation of the composite wave. (b) Find the wavelength along the direction of propagation and the wavelength transverse to the direction of propagation of the composite wave.

8.8. Show that $\langle \sin^2(\omega t - \beta z \sin\theta)\rangle$ and $\langle \sin 2(\omega t - \beta z \sin\theta)\rangle$ are equal to 1/2 and zero, respectively.

8.9. Find the spacing a for a parallel-plate waveguide having a dielectric of $\epsilon = 9\epsilon_0$ and $\mu = \mu_0$ such that 6000 MHz is 20 percent above the cutoff frequency of the dominant mode, that is, the mode with the lowest cutoff frequency.

8.10. The dimension a of a parallel-plate waveguide filled with a dielectric having $\epsilon = 4\epsilon_0$ and $\mu = \mu_0$ is 4 cm. Determine the propagating $\text{TE}_{m,0}$ modes for a wave of frequency 6000 MHz. For each propagating mode, find f_c, θ, and λ_g.

8.11. The spacing a between the plates of a parallel-plate waveguide is equal to 5 cm. The dielectric between the plates is free space. If a generator of fundamental frequency

1800 MHz and rich in harmonics excites the waveguide, find all frequencies that propagate in $TE_{1,0}$ mode only.

8.12. The electric and magnetic fields of the composite wave resulting from the superposition of two uniform plane waves are given by

$$\begin{aligned}\mathbf{E} &= E_{x0} \cos \beta_x x \cos (\omega t - \beta_z z)\, \mathbf{a}_x \\ &\quad + E_{z0} \sin \beta_x x \sin (\omega t - \beta_z z)\, \mathbf{a}_z \\ \mathbf{H} &= H_{y0} \cos \beta_x x \cos (\omega t - \beta_z z)\, \mathbf{a}_y\end{aligned}$$

(a) Find the time-average Poynting vector. (b) Discuss the nature of the composite wave.

8.13. Transverse electric modes are excited in an air dielectric parallel-plate waveguide of dimension $a = 5$ cm by setting up at its mouth a field distribution having

$$\mathbf{E} = 10\,(\sin 20\pi x + 0.5 \sin 60\pi x) \sin 10^{10}\pi t\, \mathbf{a}_y$$

Determine the propagating mode(s) and obtain the expression for the electric field of the propagating wave.

8.14. For the two-train example of Figure 8.8, find the group velocity if the speed of train numbered B is (a) 36 m/s and (b) 40 m/s, instead of 30 m/s. Discuss your results with the aid of sketches.

8.15. Find the velocity with which the group of two frequencies 2400 MHz and 2500 MHz travels in a parallel-plate waveguide of dimension $a = 2.5$ cm and having a perfect dielectric of $\epsilon = 9\epsilon_0$ and $\mu = \mu_0$.

8.16. For a narrow-band amplitude modulated signal having the carrier frequency 5000 MHz propagating in an air dielectric parallel-plate waveguide of dimension $a = 5$ cm, find the velocity with which the modulation envelope travels.

8.17. For an $\omega - \beta_z$ relationship given by

$$\omega = \omega_0 + k\beta_z^2$$

where ω_0 and k are positive constants, find the phase and group velocities for (a) $\omega = 1.5\omega_0$, (b) $\omega = 2\omega_0$, and (c) $\omega = 3\omega_0$.

8.18. By considering the parallel-plate waveguide, show that a point on the obliquely bouncing wavefront, traveling with the phase velocity along the oblique direction, progresses parallel to the guide axis with the group velocity.

8.19. For an air dielectric rectangular waveguide of dimensions $a = 3$ cm and $b = 1.5$ cm, find all propagating modes for $f = 12{,}000$ MHz.

8.20. For a rectangular waveguide of dimensions $a = 5$ cm and $b = 5/3$ cm, and having a dielectric of $\epsilon = 9\epsilon_0$ and $\mu = \mu_0$, find all propagating modes for $f = 2500$ MHz.

8.21. For $f = 3000$ MHz, find the dimensions a and b of an air dielectric rectangular waveguide such that $TE_{1,0}$ mode propagates with a 30 percent safety factor ($f = 1.30f_c$) but also such that the frequency is 30 percent below the cutoff frequency of the next higher order mode.

8.22. For an air dielectric rectangular cavity resonator having the dimensions $a = 2.5$ cm, $b = 2$ cm, and $d = 5$ cm, find the five lowest frequencies of oscillation. Identify the mode(s) for each frequency.

8.23. For a rectangular cavity resonator having the dimensions $a = b = d = 2$ cm, and filled with a dielectric of $\epsilon = 9\epsilon_0$ and $\mu = \mu_0$, find the three lowest frequencies of oscillation. Identify the mode(s) for each frequency.

8.24. In Figure 8.16, let $\epsilon_1 = 4\epsilon_0$, $\epsilon_2 = 9\epsilon_0$, and $\mu_1 = \mu_2 = \mu_0$. (a) For $\theta_t = 30°$, find θ_t. (b) Is there a critical angle of incidence for which $\theta_t = 90°$?

8.25. In Figure 8.16, let $\epsilon_1 = 4\epsilon_0$, $\epsilon_2 = 2.25\epsilon_0$, and $\mu_1 = \mu_2 = \mu_0$. (a) For $\theta_t = 30°$, find θ_t. (b) Find the value of the critical angle of incidence θ_c, for which $\theta_t = 90°$.

8.26. In Example 8.5, assume that

$$E_i = E_0(\mathbf{a}_x - \mathbf{a}_z)\cos[6\pi \times 10^8 t - \sqrt{2}\pi(x + z)]$$

and the angle of incidence is 45°. Obtain the expressions for the electric fields of the reflected and transmitted waves.

8.27. Repeat Problem 8.26 for

$$\mathbf{E}_i = E_0\,\mathbf{a}_y \cos[6\pi \times 10^8 t - \sqrt{2}\pi(x + z)]$$

8.28. In Example 8.5, assume that the permittivity ϵ_2 of medium 2 is unknown and that

$$\mathbf{E}_i = E_0\left(\frac{\sqrt{3}}{2}\mathbf{a}_x - \frac{1}{2}\mathbf{a}_z\right)\cos[6\pi \times 10^9 t - 10\pi(x + \sqrt{3}z)]$$
$$+ E_0\mathbf{a}_y \sin[6\pi \times 10^9 t - 10\pi(x + \sqrt{3}z)]$$

(a) Find the value of ϵ_2 for which the reflected wave is linearly polarized.
(b) For the value of ϵ_2 found in (a), find the expressions for the reflected and transmitted wave electric fields.

8.29. A thin-film waveguide employed in integrated optics consists of a substrate on which a thin film of refractive index (c/v_p) greater than that of the substrate is deposited. The medium above the film is air. For relative permittivities of the substrate and the film equal to 2.25 and 2.4, respectively, find the minimum bouncing angle of total internally reflected waves in the film. Assume $\mu = \mu_0$ for both substrate and film.

8.30. For a symmetric dielectric slab waveguide, $\epsilon_1 = 2.25\epsilon_0$ and $\epsilon_2 = \epsilon_0$. (a) Find the number of propagating TE modes for $d/\lambda_0 = 10$. (b) Find the maximum value of d/λ_0 for which the waveguide supports only one TE mode.

8.31. Design a symmetric dielectric slab waveguide, with $\epsilon_{r1} = 2.25$ and $\epsilon_{r2} = 2.13$, by finding the value of d/λ_0 such that the TE_1 mode operates at 20% above its cutoff frequency.

8.32. Consider the derivation of the characteristic equation for guiding of waves in the symmetric dielectric slab waveguide for the case of parallel polarization, which corresponds to TM modes. Noting that in Figure 8.18, $H_r/H_i = E_r/E_i = -\Gamma_{\|}$, where $\Gamma_{\|}$ is given by (8.75a), show that the characteristic equation is given by

$$\tan[f(\theta_i)] = \begin{cases} g(\theta_i), & m = 0, 2, 4, \ldots \\ -\dfrac{1}{g(\theta_i)}, & m = 1, 3, 5, \ldots \end{cases}$$

where

$$f(\theta_i) = \frac{\pi d\sqrt{\epsilon_{r1}}}{\lambda_0}\cos\theta_i$$

$$g(\theta_i) = \frac{\sqrt{\sin^2\theta_i - (\epsilon_2/\epsilon_1)}}{(\epsilon_2/\epsilon_1)\cos\theta_i}$$